Cannabidivarin completely rescues cognitive deficits and delays neurological and motor defects in male *Mecp2* mutant mice

Zamberletti E.[1], Gabaglio M.[1], Piscitelli F.[2], Brodie J.S.[3], Woolley-Roberts M.[3], Barbiero I.[1], Tramarin M.[1], Binelli G.[1], Landsberger N.[4], Kilstrup-Nielsen C.[1], Rubino T.[1], Di Marzo V.[2], Parolaro D.[1,5]

[1]Dept. of Biotechnology and Life Sciences (DBSV), University of Insubria, Varese, Italy; [2]Endocannabinoid Research Group, Institute of Biomolecular Chemistry, Consiglio Nazionale delle Ricerche, Pozzuoli, Naples, Italy; [3]GW Research Ltd, Cambridge (UK); [4]Dept. of Medical Biotechnology and Translational Medicine, University of Milan, Italy; [5]Zardi Gori Foundation, Milan (Italy).

Corresponding author:

Daniela Parolaro

DBSV, University of Insubria and Zardi Gori Foundation

Tel. +39 0331339417

Fax. +39 0331339459

Email daniela.parolaro@uninsubria.it

Abstract

Background: Recent evidence suggests that 2-week treatment with the non-psychotomimetic cannabinoid cannabidivarin (CBDV) could be beneficial towards neurological and social deficits in early symptomatic *Mecp2* mutant mice, a model of Rett syndrome (RTT).

Aim: To provide further insights into the efficacy of CBDV in *Mecp2*-null mice we used a lifelong treatment schedule (from 4 to 9 weeks of age) and evaluated its effect on recognition memory and neurological defects in both early and advanced stages of the phenotype progression.

Methods: CBDV 0.2, 2, 20, 200 mg/kg/day was administered to *Mecp2*-null mice from 4 to 9 weeks of age. Cognitive and neurological defects were monitored during the whole treatment schedule. Biochemical analyses were carried out in brain lysates from 9-week-old wildtype and knockout mice to evaluate brain-derived neurotrophic factor (BDNF) and insulin-like growth factor-1 (IGF-1) levels as well as components of the endocannabinoid system.

Results: CBDV rescues recognition memory deficits in *Mecp2* mutant mice and delays the appearance of neurological defects. At the biochemical level, it normalizes BDNF/IGF1 levels and the defective PI3K/AKT/mTOR pathway in *Mecp2* mutant mice at an advanced stage of the disease. *Mecp2* deletion

upregulates CB1 and CB2 receptor levels in the brain and these changes are restored after CBDV treatment.

Conclusions: CBDV administration exerts an enduring rescue of memory deficits in *Mecp2* mutant mice, an effect that is associated with the normalization of BDNF, IGF-1 and rpS6 phosphorylation levels as well as CB1 and CB2 receptor expression. CBDV delays neurological defects but this effect is only transient.

Keywords: cannabidivarin; *Mecp2* mutant mice; endocannabinoids; BDNF; IGF-1

Short title: CBDV partially relieves Mecp2-null mouse phenotype

1. Introduction

Rett syndrome (RTT) is an X-linked dominant neurodevelopmental disorder with a prevalence rate of 1 in 10,000 females. RTT patients have apparently normal perinatal development until about 6–18 months of age, after which they undergo a period of rapid regression, characterized by the appearance of autistic features, cognitive regression, stereotypic hand movements and loss of language. RTT girls also have seizures during childhood, breathing arrhythmias, develop scoliosis and lose mobility between ages 1 and 4 years (Chahrour and Zoghbi, 2007; Hagberg, 2002; Neul et al., 2014).

Mutations affecting the methyl-CpG-binding protein 2 (*MeCP2*) represent the almost exclusive cause of the disorder (Amir et al., 1999). Given the location of the *MECP2* gene on the X chromosome, males with *MECP2* mutations are more severely affected and rarely survive infancy while females, owing to X chromosome inactivation, are mosaics with cells that express either the wild-type (WT) or mutant version of *MeCP2* (Chahrour and Zoghbi, 2007).

Mecp2 deficiency in mice closely mimics the clinical features of the human disorder, including motor and neurological defects and breathing abnormalities (Ricceri et al., 2008), possibly reflecting the high conservation of the *MeCP2* amino acid sequence and the parallel dynamics of *MeCP2* expression during brain development in the two species. Thus, despite differences in brain structure

and developmental timing between humans and mice, the molecular consequences of the *MeCP2* mutation appear to be similar in the two species, and mouse models represent an essential tool for testing potential treatment strategies for RTT.

Converging evidence points to a role for endocannabinoid signaling dysregulation in the pathophysiology of neurodevelopmental conditions including social dysfunction and autism spectrum disorder (ASD) (Karhson et al., 2016; Wei et al., 2017; Zamberletti et al., 2017). Remarkably, improvement in social functioning and anxiety-like behavior was consistently reported following pharmacological modulation of different components of the endocannabinoid system in genetic and environmental models of autism (Busquets-Garcia et al., 2013; Gomis-González et al., 2016; Hosie et al., 2018; Kerr et al., 2016; Servadio et al., 2016; Jung et al., 2012; Wei et al., 2016). In line with animal data, recent human findings support a link between altered endocannabinoid activity and autism (Karhson et al., 2018) possibly suggesting that compounds acting on the endocannabinoid system could be beneficial in alleviating ASD symptoms.

Phytocannabinoids are terpenophenolic constituents of the cannabis sativa plant that, in addition to their effects on the endocannabinoid system, exhibit a range of neuromodulatory, neuroprotective, anti-oxidant and anti-inflammatory properties, including effects on biochemical pathways that could contribute to

achieve an overall therapeutic effect in major neurological disorders (Campos et al., 2016; Fernandez-Ruiz et al., 2013; Ligresti et al., 2016; Nagarkatti et al., 2009). Delta-9-tetrahydrocannabinol (THC) is the major psychotomimetic component of cannabis whose euphoric effects are mediated by the activation of CB1 receptors in the central nervous system; however, this mechanism is responsible for many untoward adverse effects, whose risk is greater with early use and high doses (Volkow et al., 2014), thus discouraging its use among children and high-risk groups. Unlike THC, other phytocannabinoids with weak or no psychotropic activity seem to hold great yet unexplored promise as therapeutic agents for complex and multifaceted neurodevelopmental diseases. Cannabidiol (CBD) and cannabidivarin (CBDV) are both effective in ameliorating epilepsy (Brodie and Ben-Menachem, 2017) and motor dysfunctions (Iannotti et al., 2018), two conditions frequently observed also in RTT patients (Steffenburg et al., 2001; Huppke et al., 2007), supporting their potential as treatment options for RTT. Accordingly, a recent paper showed that a 2-week long treatment schedule with CBDV could be beneficial towards neurological and social deficits in early symptomatic *Mecp2* mutant mice, a model for RTT, possibly via its action at GPR55 receptors (Vigli et al., 2018). Both CBD and CBDV activate and desensitize TRPV1 cation channels and modulate anandamide uptake. Additionally, CBDV also modulates the levels of the endocannabinoid 2-AG (De

Petrocellis et al., 2011; 2012), which is crucially involved in synaptic plasticity and cognitive processes (Zhang et al., 2014).

To gain more insight into the possible efficacy of CBDV in the context of RTT, in this study we provided additional pieces of data by testing the effect of similar doses of CBDV in another animal model of RTT, namely *Mecp2*-null mice, using a lifelong treatment schedule (from 4 to 9 weeks of age). CBDV effects on recognition memory and neurological deficits were monitored throughout the entire animals' lifespan. At an advanced stage of the phenotype progression (9-week old mice), biochemical analysis were performed to assess whether CBDV could modulate neurochemical abnormalities that are found in the brain of *Mecp2*-null mice. In particular, we investigated CBDV's effect on brain-derived neurotrophic factor (BDNF), insulin-like growth factor-1 (IGF-1) and their common downstream PI3K/Akt/mTOR signaling pathway whose reduced levels have been implicated in the disease progression (Castro et al., 2014; Li and Pozzo-Miller, 2014; Ricciardi et al., 2011) and we analyzed nuclear volumes in the layer V of the medial prefrontal cortex (mPFC) and CA1 region of the hippocampus, whose reduction represents a consistent feature of *Mecp2* deficiency at the cellular level (Gadalla et al., 2013; Giacometti et al., 2007). Finally, given that altered endocannabinoid activity contributes to the pathogenesis of several psychiatric conditions including anxiety-related disorders, intellectual disabilities, major

motor disorders, seizures and autism (Campolongo and Trezza, 2012; Fernández-Ruiz and Gonzáles, 2005; Katona, 2015; Zamberletti et al., 2017), we investigated the status of components of the endocannabinoid system, in terms of endocannabinoid levels, enzymatic machinery and CB1, CB2 receptors.

2. Experimental procedures

2.1.1 Animals

We used the CD1 *Mecp2*-null mouse strain described in Cobolli Gigli et al. (2016). All experimental procedures were carried out in male *Mecp2* WT and KO mice, housed in groups of 4-5 in clear plastic cages (33.1x15.9x13.2 cm) on a 12 h light-dark cycle (lights on 8:00 AM) and in a temperature- (22 ± 2°C) and humidity-controlled environment (50 ± 10%) with a plastic tube for environmental enrichment and free access to food and water. Experimental procedures were performed in accordance with the guidelines released by the Italian Ministry of Health (D.L. 2014/26) and the European Community directives regulating animal research (2010/63/EU). Protocols were approved by the Italian Minister for Scientific Research and all efforts were made to minimize the number of animals used and their suffering.

2.1.2 Breeding procedure and genotyping

Wild-type CD1 males and *Mecp2*$^{+/-}$ heterozygous CD1 females aged between 2 and 4 months were mated for four days. Dams gave birth and raised their litters

until weaning. Litters were not culled and no selection other than genotype was made. Mouse genotypes were determined through PCR on genomic DNA purified from tail biopsy. Biopsies were obtained within the third and fourth week of life. Forward PCR primer sequences: 5'-CCATGCGATAGGCTTGATGA for the identification of the null allele, 5'-GACCCCTTGGGACTGAAGTT for the wt allele. Common reverse primer sequence: 5'-CCACCCTCCAGTTTGGTTTA . The obtained PCR products were: a single band of 450 base pairs (bp) for the Mecp2-null mice; a single band of 400 bp for the wt animals and the two bands for heterozygous females.

2.2 Treatment

A total of 112 littermate male mice from 4 different cohorts were used in the study. Based on the available litters at weaning, animals were randomly divided into 10 treatment groups: 22 for WT-vehicle, 10 for WT-CBDV 0.2 mg/kg, 13 for WT-CBDV 2 mg/kg, 12 for WT-CBDV 20 mg/kg, 3 for WT-CBDV 200 mg/kg, 11 for KO-vehicle, 6 for KO-CBDV 0.2 mg/kg, 13 for KO-CBDV 2 mg/kg, 14 for KO-CBDV 20 mg/kg and 8 for KO-CBDV 200 mg/kg.

Purified CBDV (96.4%; CBD 3.6%) was provided by GW Research (Cambridge, UK), stored at -20°C and freshly prepared daily by dissolution in ethanol, kolliphor EL and saline (2:1:17). The treatments started at PND 28 (week 4) and lasted until PND 67 (week 9). Mice received a daily intraperitoneal injection of CBDV (or

vehicle) at the doses of 0.2, 2, 20 or 200 mg/kg between 9:00 am and 11:00 am based on previous pharmacokinetic (Deiana et al., 2012) and in vivo (Vigli et al., 2018) studies.

2.3 Behavioral studies

Behavioral testing was carried out by two observers blind to the treatment conditions. The timeline of the experiments is reported in supplementary figure S1.

2.3.1 Score test

Neurological defects in *Mecp2*-null mice were evaluated using observational scoring for hindlimb clasping, gait, breathing, tremor, mobility and general condition. Starting from PND 28, *Mecp2* WT and KO mice were scored every other day to evaluate the effect of CBDV treatment on motor symptoms, neurological signs and general condition. Score data were expressed as the weekly average of four-day observations in each corresponding week. Each of the six symptoms was scored from 0 to 2 (0 corresponds to the symptom being absent or the same as in the WT animal; 1 when the symptom was present; 2 when the symptom was severe) as previously described (Guy et al., 2007; Szczesna et al., 2014; see Supplementary Methods for a detailed description). Whenever a mouse scored 2 out of 2 in the three criteria tremor, breathing,

general condition, or lost 20% of its body weight during the experiment, it was killed by cervical dislocation.

2.3.2 Novel object recognition (NOR) test

The test was performed on PND 41, 56 and 66. The experimental apparatus used for the NOR test was an open-field box (43x43x32 cm) made of Plexiglas, placed in a dimly illuminated room. Animals performed each test individually as in Zamberletti et al. (2015). Each animal was placed in the arena and allowed to explore two identical previously unseen objects for 10 minutes (familiarization phase). The test phase was performed after an inter-trial interval of 30 minutes. During the test phase, the time spent exploring the familiar object (Ef) and the new object (En) was recorded separately by two observers blind to the groups and the discrimination index was calculated as follows: (En-Ef)/(En+Ef) x 100. Objects were changed in subsequent testing sessions of the NOR test.

2.4 Biochemical studies

2.4.1 Western blot

Mice having all the same age (9 weeks old) were sacrificed by cervical dislocation 24 hours after the last CBDV (or vehicle) injection. The brains were quickly removed, frozen in liquid nitrogen and stored at -80°C.

50 µg of total protein lysates from hemisected brains were run on a SDS-polyacrylamide gel. The proteins were transferred to polyvinylidene difluoride

(PVDF) membranes and blocked for 2 hours before incubation overnight at 4°C with specific primary antibodies (listed in supplementary Table S1). Bound antibodies were detected with horseradish peroxidase (HRP) conjugated secondary anti-rabbit or anti-goat antibody (1:2000-1:5000; Chemicon International, Temecula, CA). The blots were normalized against mouse anti-β-actin monoclonal antibody (1:10000; Sigma Aldrich, Italy), rabbit polyclonal anti-totalAKT (1:1000; Abcam, Cambridge, UK), rabbit polyclonal anti-totalS6 (1:1000; Cell Signaling, Danvers, MA) or rabbit polyclonal anti-totalERK1/2 (1:1000; Cell Signaling, Danvers, MA). Bound antibodies were visualized using Clarity Western ECL Substrate (Bio-Rad Laboratories, Hercules, CA, USA) and bands were detected with a GBOX XT camera (Syngene, Cambridge, UK). Optical density of the bands was quantified using Image Pro Plus 7.0 software (MediaCybernetics, Bethesda, MD, USA), normalized and expressed as arbitrary units.

2.4.2 Lipid extraction and endocannabinoid measurement

Hemisected brains were dounce-homogenized and extracted with acetone containing internal deuterated standards for anandamide (AEA), palmitoylethanolamide (PEA), oleoylethanolamide (OEA) and 2-arachidonoylglycerol (2-AG) quantification by isotope dilution LC-MS, i.e. 5 pmol d8-AEA, and 50 pmol d4-PEA, d4-OEA, and d5-2-AG, (Cayman Chemical), respectively. The lipid-containing organic phases were then purified by open bed

chromatography on silica and fractions were obtained by eluting the column with 99:1, 90:10, and 50:50 (v/v) chloroform/methanol. Fractions eluted with chloroform/methanol 90:10 were collected, the excess solvent evaporated with a rotating evaporator, and aliquots analyzed by isotope dilution-LC/atmospheric pressure chemical ionization/MS carried out in the selected ion monitoring mode by using a Shimadzu HPLC apparatus (LC-10ADVP) coupled to a Shimadzu (LCMS-2020) quadrupole mass spectrometer via a Shimadzu atmospheric pressure chemical ionization interface. MS detection was performed by using values of m/z 356 and 348 (molecular ions + 1 for d8-AEA and AEA), m/z 304 and 300 (molecular ions + 1 for d4-PEA and PEA), m/z 330 and 326 (molecular ions + 1 for d4-OEA and OEA) and m/z 384 and 379 (molecular ions +1 for d5-2-AG and 2-AG). AEA, PEA, OEA, and 2-AG levels were therefore calculated on the basis of their area ratios with the internal deuterated standard signal areas. Lipid amounts expressed as pmol were then normalized per gram or milligram of wet tissue.

2.4.3 Immunohistochemistry

Frozen brain sections were obtained using a Leica cryostat CM1510 set to 20μm thickness and a −20°C chamber temperature. Sagittal sections were collected on gelatin-coated slides (4 sections per slide, 200μm apart) and permeabilized with 100% methanol at -20°C for 30 minutes. After three washes in 0.05% Triton X-

100 in TBS, sections were blocked with 3% normal goat serum in TBS for 1 hour at room temperature and then incubated overnight 4°C with rabbit anti-phospho-rpS6 (Ser240/244) (1:50) from Cell Signaling Technology (Danvers, MA, USA) diluted in blocking solution. After blocking peroxidase activity with 0.3% H_2O_2 in TBS for 15 min, sections were washed in TBS and incubated for 4 hours at room temperature with goat anti-rabbit horseradish peroxidase (HRP) conjugated secondary antibody diluted 1:100 (Vector Labs, Burlingame, CA, USA). The sections were then incubated in chromogen 3,3'-diaminobenzidine tetrahydrochloride (DAB) for 5 min. The reaction was stopped in PBS, sections were dehydrated and cover slipped.

Digital Images were captured using Retiga R1 CCD camera (QImaging, Surrey, BC, Canada) attached to an Olympus BX51 (Tokyo, Japan) polarizing/light microscope. Ocular imaging software (QImaging) was used to import images from the camera. Images of layer V neurons in the medial prefrontal cortex were acquired by first delineating the brain sections and the regions of interest (ROI) at low magnification (×4 objective) and the ROI were further refined under a ×40 objective. Labeled cells were counted manually in every ten 20μm-thick sagittal section (200μm apart) within the ROI using a 300 × 300 μm grid as reference. Three mice per each experimental group (four sections/mouse) were analyzed blinded.

2.4.4 Nuclear size measurements

For DAPI staining, slides were pre-incubated in 80% Methanol at 4°C for 5 min, washed in TBS for 10 min and then incubated in a working solution 1 to 10 in PBS from a 0.01% stock solution in the dark for 30 minutes at room temperature. After several washes in PBS, sections were dehydrated and cover slipped. Images of layer V neurons in the medial prefrontal cortex and of CA1 pyramidal cell layer were acquired using a ×20 objective after having defined the outlines of the regions of interest at low magnification (×4 objective). Outlines of nuclei were manually traced at ×20 image magnification using ImageJ software (NIH, Bethesda, MD, USA). Four slices of tissue from three animals per each experimental group (30–75 cells/animal) were analyzed blind to the treatment groups. Only in-focus neurons that were completely within the field of view and whose signal was not occluded by overlying cells were measured.

2.5 Statistics

The Shapiro–Wilk test was first used to determine if the data were normally distributed. Qualitative non-normally distributed score data were analyzed non-parametrically using Pearson's Chi-square test with Yates correction. NOR data and biochemical results were expressed as mean ± SEM and analyzed by two-way repeated measures and main effects ANOVA, respectively, by the GLM package of Statistica 7.0. Bonferroni’s post-hoc test was used to control for

multiple comparisons. Kaplan-Meier survival curves were generated and compared using a Dunnet-type log-rank method. The level of statistical significance was set at $p<0.05$. Calculations were carried out using Statistica 7.0 and R (R Core Team, 2013) Statistical Software.

3. Results

3.1 Behavioral data

3.1.1 Effect of chronic CBDV treatment on motor and neurological sign progression in Mecp2-deficient male mice

Figure 1A shows the effect of chronic CBDV treatment on tremors, hind limb clasping, breathing, gait, mobility and general condition in KO mice over time. No symptoms were present in *Mecp2* KO mice until 4 weeks of age (data not shown). Either WT mice treated with vehicle or CBDV did not show any symptom (score = 0) during the entire period of observation (data not shown).

Male *Mecp2* KO mice exhibited tremors beginning from 5 weeks of age. CBDV administration significantly reduced tremors in *Mecp2* KO mice at 5 ($\chi^2_{[8]3.}$ =12.765, p=0.012) and 6 ($\chi^2_{[8]}$ =16.422, p=0.036) weeks of age, but not later. Doses of 2, 20 and 200 mg/kg showed similar efficacy ($p<0.001$) whereas the lowest dose of CBDV tested, 0.2 mg/kg, was ineffective.

Mecp2 KO mice showed a significant increase in hind limb clasping starting from 6 weeks of age. CBDV treatment significantly attenuated hind limb clasping in KO

mice at 6 weeks of age ($\chi^2_{[8]}$=22.814, p=0.0036). This effect was reached at doses of 2 (p>0.05), 20 (p<0.01) and 200 mg/kg (p<0.05). In contrast, CBDV was ineffective at the lowest dose tested, 0.2 mg/kg.

Breathing and gait abnormalities were evident in *Mecp2* KO mice starting from 7 weeks of age. Breathing ($\chi^2_{[8]}$=22.405, p=0.0042) and gait ($\chi^2_{[8]}$=16.275, p=0.039) were improved by CBDV in *Mecp2* KO mice at 7 weeks of age. CBDV treatment attenuated breathing abnormalities at doses of 2 (p<0.01), 20 (p<0.05) and 200 (p<0.05) mg/kg compared to KO-vehicle mice. Similarly, gait alterations were significantly reduced by CBDV treatment at doses of 2 (p<0.01), 20 (p<0.01) and 200 (p<0.001) mg/kg. Again, the lowest dose tested was completely ineffective.

Impaired mobility and deterioration of general condition in KO mice was observed starting from 7 weeks of age. CBDV administration at all doses tested did not affect both parameters in KO mice during the whole treatment schedule.

To gain an overall impression of CBDV treatment in *Mecp2* KO mice over time, individual behavior scores were combined into a total symptom score for each mouse (figure 1B). Total symptom score was significantly increased in KO mice treated with vehicle starting from 5 weeks of age compared to WT mice and continued to increase until the end of the observation period. Significant effects were observed on total symptom score at 6 ($\chi^2_{[8]}$=19.617, p=0.0037) and 7 (χ^2

$_{[8]}$=21.732, p=0.0041) weeks of age. Treatment with CBDV 2, 20 and 200 mg/kg showed similar efficacy in attenuating motor and neurological deficits in KO mice. Indeed, they significantly improved total symptom score in KO mice at 6 ($p<0.001$) and 7 ($p<0.001$) weeks of age, although CBDV's beneficial effect was lost at later stages of the disease progression (i.e. 8 and 9 weeks of age). In contrast, CBDV 0.2 mg/kg did not affect the progression of symptoms over the entire observation period.

3.1.2 Effect of chronic CBDV treatment on survival and body weight in Mecp2-deficient male mice

Survival data refer to all mice that underwent behavioral assessment. Figure 2A shows the percentage survival of *Mecp2* KO and WT mice treated with CBDV or vehicle. The results are plotted as Kaplan–Meier survival curves and expressed as the percentage of surviving mice over total mice with respect to time for each experimental group. No lethality was observed in WT mice treated with either vehicle or CBDV. In contrast, survival in KO mice treated with vehicle was only 38.5% by 9 weeks of age. All doses of CBDV showed a trend to increase survival rates in *Mecp2* KO mice at the end of the observation period compared to vehicle-treated littermates (KO-CBDV 0.2 mg/kg: 66.6%; KO-CBDV 2 mg/kg: 61.5%; KO-CBDV 20 mg/kg: 71.4%; KO-CBDV 200 mg/kg: 87.5%), although this effect

reached statistical significance only at the highest dose tested, 200 mg/kg (p=0.0433; log Rank test).

Regarding body weight, as expected, *Mecp2* KO mice were significantly leaner than WT littermates (figure 2B). Chronic CBDV administration did not recover body weight in KO mice, although a post-hoc test did not reveal significant differences between WT-vehicle and KO mice treated with CBDV 2/20/200 mg/kg.

3.1.3 Effect of chronic CBDV treatment on recognition memory deficits in Mecp2-deficient male mice

Figure 3 shows the effect of chronic CBDV administration on short-term recognition memory at PND 41, 56 and 66. No differences in exploratory behavior and locomotor activity were observed in WT and KO mice during the training session of the recognition memory test (Supplementary Figure S2). Exploration times of the novel object and the familiar object in the test phase are reported in Supplementary Figure S3. Repeated measures ANOVA with time as the dependent variable revealed significant main effects of genotype ($F_{[1-244]}$=111.5, p<0.0001), treatment ($F_{[4-244]}$=47.77, p<0.0001) and genotype x treatment interaction ($F_{[8-244]}$=4.152, p=0.0440) on recognition memory. A cognitive impairment in recognition memory was consistently present in KO mice and was maintained until adulthood. KO animals showed significant reductions of the

discrimination index at PND 41 ($p<0.001$), 56 ($p<0.001$) and 66 ($p<0.001$) compared to WT mice. At each time point, administration of CBDV 2, 20 and 200 mg/kg significantly counteracted the cognitive impairment in recognition memory present in KO mice ($p<0.001$). In contrast, chronic CBDV treatment at the lowest dose tested, 0.2 mg/kg, did not rescue the cognitive impairment in KO mice.

3.2 Biochemical data

3.2.1 Effect of chronic CBDV treatment on BDNF, IGF-1 protein levels and downstream PI3K/AKT/mTOR and ERK1/2 pathways in hemisected brains of Mecp2-deficient male mice

CBDV at all doses tested did not affect the expression of all the considered biochemical markers when given chronically to WT mice.

Statistical analysis showed significant effects of genotype ($F_{[1,38]}=5.677$, $p=0.0220$), treatment ($F_{[4,38]}=2.677$, $p=0.0455$) and genotype x treatment interaction ($F_{[4,38]}=9.997$, $p=0.0081$) on BDNF expression. BDNF protein levels were significantly reduced in *Mecp2* KO mice treated with vehicle or CBDV 0.2 mg/kg with respect to WT littermates ($p<0.01$; $p<0.05$ respectively). In contrast, 2, 20 and 200 mg/kg CBDV significantly restored BDNF levels in KO mice, to a similar degree ($p<0.05$; Figure 4A).

Two-way ANOVA analysis revealed significant effects of genotype ($F_{[1,38]}=4.773$, $p=0.0032$) and genotype x treatment interaction ($F_{[4,38]}=2.709$, $p=0.0444$) on IGF-

1 levels. IGF-1 levels were significantly reduced in *Mecp2* KO mice treated with vehicle compared to WT animals ($p<0.05$). CBDV significantly increased IGF-1 levels in KO mice at doses of 2 ($p<0.05$), 20 ($p<0.05$) and 200 ($p<0.01$) mg/kg (Figure 4A).

A significant genotype x treatment interaction ($F_{[4,26]}=6.574$, $p=0.0009$) and a trend for genotype effect ($F_{[1,26]}=3.967$, $p=0.0570$) were found on pAKT levels (figure 4B). pAKT was significantly reduced in *Mecp2* KO mice treated with vehicle compared to WT-vehicle animals ($p<0.05$). Chronic CBDV administration dose dependently recovered pAKT levels in *Mecp2* deficient mice, reaching statistical significance at doses of 20 ($p<0.01$) and 200 ($p<0.001$) mg/kg.

Significant effects of genotype ($F_{[1,29]}=23.83$, $p<0.0001$) and genotype x treatment interaction ($F_{[4,29]}=2.702$, $p=0.0500$) on rpS6 phosphorylation were also observed. *Mecp2* deletion significantly reduced rpS6 phosphorylation within the adult brain ($p<0.001$). Chronic CBDV treatment significantly increased rpS6 phosphorylation levels in KO mice compared to vehicle-treated mutants at doses of 2 ($p<0.05$), 20 ($p<0.01$) and 200 ($p<0.05$) mg/kg.

Immunohistochemical analysis revealed significant effects of genotype ($F_{[1,20]}=12.07$; $p=0.0024$), treatment ($F_{[4,20]}=3.042$; $p=0.0413$) and genotype x treatment interaction ($F_{[4,20]}=7.156$; $p=0.0010$) on rpS6 phosphorylation in layer V neurons of the medial prefrontal cortex (figure 4C). Indeed, rpS6 phosphorylation

was significantly decreased in *Mecp2* KO mice compared to WT animals ($p<0.05$); CBDV administration significantly enhanced rpS6 phosphorylation in mutant mice at doses of 20 ($p<0.05$) and 200 ($p<0.01$) mg/kg without affecting its levels in WT animals. A trend towards an enhancement of rpS6 phosphorylation was also present in KO mice after administration of the 2 mg/kg dose ($p=0.0717$) whereas the 0.2 mg/kg dose was completely ineffective.

Finally, neither genotype nor CBDV treatment affected ERK1/2 phosphorylation (figure 4B).

3.2.2 CBDV effect on nuclear areas in Layer V neurons of the medial prefrontal cortex and in the CA1 layer of the hippocampus

In the mPFC, the mean nuclear area of KO neurons was 35.5% smaller than that of WT neurons (WT-vehicle = 69.98 ± 2.091 μm^2, KO-vehicle = 45.10 ± 1.208 μm^2; $p<0.001$, Figure 5A). CBDV treatment, at all doses tested, did not affect nuclear size in KO neurons (CBDV 0.2 mg/kg = 40.48 ± 1.598 μm^2, CBDV 2 mg/kg = 47.71 ± 1.779 μm^2, CBDV 20 mg/kg = 48.44 ± 1.782 μm^2, CBDV 200 mg/kg = 53.08 ± 2 μm^2). In the CA1 layer of the hippocampus, the mean nuclear area of KO neurons was 32.3% smaller than that of WT neurons (WT-vehicle = 63.5 ± 2.237 μm^2, KO-vehicle = 43.0 ± 1 μm^2; $p<0.001$, Figure 5B). A partial rescue of hippocampal neurons nuclear size was observed in KO mice after chronic CBDV administration at doses of 2, 20 and 200 mg/kg (CBDV 2 mg/kg =

53.46 ± 1.721 μm^2, CBDV 20 mg/kg = 52.55 ± 1.982 μm^2, CBDV 200 mg/kg = 51.66 ± 1.650 μm^2), but not 0.2 mg/kg (CBDV 0.2 mg/kg = 47.26 ± 1.862 μm^2).

3.2.3 Effect of chronic CBDV treatment on cannabinoid CB1 and CB2 receptors in Mecp2-deficient male mice

Two-way ANOVA analysis revealed significant effects of genotype and genotype x treatment interaction on CB1 ($F_{[1,32]}$=19.89, p<0.0001; $F_{[4,32]}$=3.429, p=0.0193) and CB2 ($F_{[1,32]}$=4.662, p=0.0384; $F_{[4,32]}$=3.834, p=0.0118) receptors (figure 6). CB1 levels were significantly increased in *Mecp2* KO mice treated with vehicle compared to WT-vehicle littermates (p<0.001). Chronic CBDV treatment significantly reduced CB1 receptor expression in KO mice at doses of 2 (p<0.05), 20 (p<0.05) and 200 (p<0.05) mg/kg. CBDV at all doses tested did not affect CB1 receptor levels when chronically administered to WT animals. CB2 receptor expression was significantly enhanced in *Mecp2* KO mice treated with vehicle compared to WT-vehicle controls (p<0.001). Chronic CBDV administration significantly rescued CB2 receptor expression in KO mice at doses of 2 (p<0.001), 20 (p<0.001) and 200 (p<0.001) mg/kg, without affecting its levels in WT littermates.

3.2.4 Effect of chronic CBDV treatment on endocannabinoid contents in Mecp2-deficient male mice

No statistically significant differences in AEA, OEA PEA and 2-AG levels were found between the two genotypes, although a trend for the increase of AEA ($p=0.0613$) and OEA ($p=0.0817$) was noticed in KO mice (figure 7A). Statistical analysis revealed significant effects of genotype x CBDV treatment interaction on AEA ($F_{[4,20]}=5.859$, $p=0.045$) and 2-AG ($F_{[4,20]}=5.375$, $p=0.041$) levels as well as non-significant trend on OEA ($F_{[4,20]}=8.787$, $p=0.067$) content. CBDV administration at doses of 2 ($p<0.05$), 20 ($p<0.001$) and 200 ($p<0.01$) mg/kg significantly increased AEA levels in *Mecp2* KO mice with respect to WT-vehicle mice. A similar effect of CBDV was also observed on OEA levels. Indeed, CBDV at 2 ($p<0.01$), 20 ($p<0.001$) and 200 ($p<0.05$) mg/kg significantly enhanced OEA content. Chronic CBDV administration significantly reduced 2-AG levels in the brain of KO mice at doses of 20 ($p<0.05$) and 200 ($p<0.01$) mg/kg compared to vehicle-treated animals. CBDV treatment also showed a trend toward reduction of 2-AG levels in WT mice. Finally, CBDV treatment did not affect PEA content in the brain of both WT and KO animals.

3.2.5 Effect of chronic CBDV treatment on endocannabinoid synthetic and degrading enzymes in Mecp2-deficient male mice

Two-way ANOVA analysis revealed significant effects on NAPE-PLD (genotype, $F_{[1,32]}=5.724$, $p=0.0228$; genotype x treatment interaction, $F_{[4,32]}=3.227$, $p=0.0247$), FAAH (genotype, $F_{[1,32]}=11.14$, $p=0.0022$; treatment, $F_{[4,32]}=1.782$,

p=0.1576) and DAGLα (treatment, $F_{[4,32]}$=11.75, p<0.0001) levels in the brains of KO mice (figure 7B). The expression of the main AEA synthetic enzyme NAPE-PLD was significantly increased in male *Mecp2* KO mice after chronic treatment with CBDV at the highest dose tested (p<0.01). In contrast, CBDV treatment at the lowest doses did not affect NAPE-PLD levels both in *Mecp2* WT and KO mice. Deletion of *Mecp2* resulted in a significant reduction of FAAH levels (p<0.05) that were not rescued by chronic CBDV administration. In addition, chronic treatment with CBDV showed a trend towards a reduction in FAAH expression in WT mice at doses of 0.2 and 20 mg/kg. CBDV treatment also affected the expression of DAGLα, a key enzyme in the biosynthesis of the endocannabinoid 2-AG. In fact, chronic CBDV administration significantly reduced DAGLα protein levels at all doses tested both in WT (p<0.01) and in KO (p<0.001) mice. No effect of either genotype or CBDV treatment was observed on the 2-AG degrading enzyme MAG lipase.

3.2.6 Protein levels of BDNF, p-rpS6, endocannabinoid receptors and enzymes in the brain of pre-symptomatic 4-week-old mice

In order to establish whether the expression of BDNF, p-rpS6 as well as endocannabinoid receptors and synthetic/degrading enzymes was altered in an apparently asymptomatic phase of the phenotype progression, we performed Western blot analysis in brain lysates from 4-week-old WT and KO mice, i.e.

before starting CBDV treatment. As reported in supplementary figure S4, both BDNF and rpS6 phosphorylation levels were significantly reduced in 4-week-old *Mecp2*-null mice compared to WT animals by about 48.3% and 35.9% respectively. In contrast, no alteration in the expression of CB1 and CB2 receptors was present at this stage of the phenotype progression. Similarly, no changes were found in the main endocannabinoid synthetic and degrading enzymes, although a trend towards a reduction in MAG lipase expression was present (p=0.0805).

4. Discussion

Chronic administration of the non-psychotomimetic phytocannabinoid CBDV completely recovers recognition memory deficits in *Mecp2* KO animals and this improvement persists at advanced stages of the phenotype progression. Furthermore, CBDV prolongs survival and delays the appearance of neurological and motor signs in *Mecp2* KO mice in a time window between 6 and 7 weeks of age. This last effect is in line with previous findings by Vigli et al. (2018) showing that 14 days of treatment with similar doses of CBDV improves the general health status, the social sphere and the motor skills in *MeCP2*-308 male mice. However, our study provides additional information supporting that CBDV's beneficial effect on motor and neurological signs is only transient and is lost when a longer treatment schedule (5 weeks long) is applied. Thus, the effect of CBDV might be

explained better as a delay in the onset of the neurological defects rather than a reduction in their intensity at a specific age.

From a pharmacological point of view, CBDV does not show a linear dose-response curve but it elicits an “all-or-none” response, as doses of 2, 20 and 200 mg/kg show similar efficacy in ameliorating the phenotype of *Mecp2* mutant mice, whereas the lowest dose tested, 0.2 mg/kg, is completely ineffective. Although a steep dose-response effect might exist between 0.2 and 2 mg/kg, CBDV’s non-linear dose response curve could be a consequence of drug tolerance following repeated exposure or target desensitization. However, a final explanation must await the identification of the specific target responsible for CBDV’s effects in this model. In addition, we cannot rule out the possibility that CBD content in our preparation, which is primarily CBDV (96.4%), but also contains low levels of CBD (3.6%), might have affected CBDV pharmacokinetics. In fact, different dose-response curves can be observed when cannabinoids are administered in isolation or in combinations that contain also low levels of other phytocannabinoids (Gallily et al., 2015; Zuardi et al., 2017).

Also, we cannot exclude that CBD could participate in the overall effects of drug treatment reported in this study, as significant neuroprotective effects of this phytocannabinoid were reported in conditions including depression, anxiety, stroke and neurodegenerative diseases even at very low doses (Campos et al.,

2017; Crippa et al., 2018) and low doses of CBD improved cognition, motor activity and BDNF levels in animal models (Avraham et al.,2011; Magen et al., 2010).

Biochemical studies performed at an advanced stage of the phenotype shows that CBDV treatment simultaneously elevates the levels of BDNF and IGF-1 in the brain of clearly symptomatic *Mecp2* KO mice at behaviorally efficacious doses.

Expression of BDNF is decreased in mouse models of RTT (Chang et al., 2006; Chen et al., 2003; Li and Pozzo-Miller, 2014; Martinowich et al., 2003) and enhancement of BDNF levels in vivo relieves some symptoms of the mutant phenotype (Chang et al., 2006; Deogracias et al., 2012; Johnson et al., 2012; Kline et al., 2010; Kron et al., 2014; Ogier et al., 2007; Roux et al., 2012; Schmid et al., 2012). Unfortunately, the therapeutic potential of BDNF is limited by its poor efficiency at crossing the blood–brain barrier (Pardridge et al., 1994). Hence, possible therapeutic strategies must rely on the identification of agents capable of indirectly stimulating BDNF levels. Remarkably, our data support CBDV potential to modulate BDNF levels in *Mecp2*-null mice.

CBDV treatment also increases IGF-1 levels in the brain of mutant mice. IGF-1 is another neurotrophic factor that holds great promise as therapeutic agent in RTT. Like BDNF, IGF-1 is widely expressed in the brain during development

(Dyer et al., 2016). In mouse models, administration of both IGF-1 and its truncated form (1-3)IGF-1 reverses many of the features of the RTT phenotype (Castro et al., 2014; Chen and Russo-Neustadt, 2007; Della Sala et al., 2016; Tropea et al., 2009) and early studies in RTT patients have demonstrated the tolerability and safety of IGF-1 as a potential treatment (Khwaja et al., 2014; Pini et al., 2016; Pini et al., 2014; Pini et al., 2012).

Although both BDNF and IGF-1 signal via PI3K/AKT and MAPK/ERK pathways to affect neuronal maturation and survival (Tropea et al., 2006; Yoshii and Constantine-Paton, 2007; Zheng and Quirion, 2004), there is direct evidence of the involvement of the AKT pathway in RTT. Reduced phosphorylation of rpS6 in *Mecp2* deficient mice is specific to signaling via AKT and not ERK1/2 kinases (Ricciardi et al., 2011). Worth noting, CBDV-mediated increases of BDNF and IGF-1 are associated with the normalization of their common downstream AKT/mTOR signaling pathway whereas no effects of either genotype or CBDV treatment are observed on ERK1/2 expression. Interestingly, reduced phosphorylation of rpS6 in *Mecp2* deficient mice is most intense in the mPFC, in line with recent studies supporting a contribution of mPFC hypofunction to the development of RTT-like phenotypes (Howell et al., 2018; Sceniak et al., 2016). In particular, excitatory hypoconnectivity in the mPFC has been linked to cognitive impairments in *Mecp2* mutant mice (Howell et al., 2018) possibly suggesting that

CBDV's ability to normalize rpS6 phosphorylation in the mPFC could contribute to its beneficial effect on memory impairments. Consistent with this hypothesis, the normalization of PI3K/AKT/mTOR pathway after CBDV administration is observed at a time point when CBDV is still recovering memory deficits but is no longer effective towards motor and neurological signs (i.e. 9 weeks of age).

As reduction of nuclear volumes represents a consistent feature of *Mecp2* deficiency at the cellular level (Gadalla et al., 2013; Giacometti et al., 2007), we assessed whether CBDV treatment could affect this parameter. Analysis of nuclear volumes indicates that CBDV did not rescue nuclear size in the layer V of the mPFC and only a partial effect was observed in the CA1 area of the hippocampus of *Mecp2* mutant mice, suggesting CBDV's inability to recover this morphological alteration at least at the end of the treatment schedule.

A previous study found increased levels of GPR55 receptor in RTT mouse hippocampus (Vigli et al., 2018), hence we here checked for possible changes on other components of the endocannabinoid system. Interestingly, the expression of brain CB1 and CB2 receptors is up-regulated in *Mecp2* deficient mice and chronic CBDV treatment at doses of 2, 20 and 200 mg/kg significantly normalized the levels of both receptors at this advanced stage of the phenotype progression. Given that CBDV binds to CB1 and CB2 receptors with very weak affinity (Amada et al., 2013; Hill et al., 2012a; Hill et al., 2013; Iannotti et al., 2014;

Rosenthaler et al., 2014), we hypothesize that normalization of CB1 receptor expression following CBDV treatment in *Mecp2* KO mice might occur indirectly as a consequence of its ability to modulate endocannabinoid signaling, namely by increasing AEA levels and hence down-regulating cannabinoid receptor expression. Indeed, chronic CBDV administration at doses of 2, 20 and 200 mg/kg increased AEA levels and elevates OEA content in *Mecp2* mutant mice, effects that are associated with reduced FAAH expression and, only for the highest dose tested, i.e. 200 mg/kg, with enhancement of NAPE-PLD expression. Furthermore, CBDV greatly reduced 2-AG levels both in WT and KO mice. This effect might be exerted at least in part via reduction of DAGLα expression, although the doses that were more efficacious at reducing 2-AG levels were also the ones least efficacious at exerting this effect. It is possible that CBDV reduces 2-AG levels also via its previously reported ability to inhibit DAGLα activity in vitro (Bisogno et al., 2003; De Petrocellis et al., 2011). Thus, in our experimental conditions CBDV is associated with enhancement of AEA and OEA levels likely through inhibition of FAAH and reduction of 2-AG, possibly in part through inhibition of DAGLα.

Up-regulation of CB1 and CB2 receptors and down-regulation of FAAH levels were also present in naïve 9-week-old *Mecp2* KO mice (see supplementary figure

S5), indicating that these changes did not arise from chronic handling procedure (Sciolino et al., 2010).

It is not possible from our data to draw any conclusion as to whether alterations of the endocannabinoid system in *Mecp2* mutant mice sustain the phenotype or represent a compensatory mechanism. Similarly, further studies are needed in order to assess whether CBDV effects on the components of the endocannabinoid (AEA and 2-AG) and endocannabinoid-related (OEA) signaling systems are a mere consequence or, instead, contribute to its therapeutic effect. The observation that, unlike BDNF and p-rpS6, endocannabinoid receptors and endocannabinoid enzymatic machinery are not altered in the brain of apparently asymptomatic 4-week-old *Mecp2* KO mice possibly suggests that the expression of the different components of the endocannabinoid system could be dynamically regulated during phenotype progression in *Mecp2* KO mice. However, any conclusion on the role of the endocannabinoid system in this animal model must await the investigation of the effects of drugs specifically targeting the single components of the system both at baseline and following CBDV treatment.

Two major limitations should be taken into account when interpreting results from this study. First, Western blot experiments were carried out on hemibrains rather than discrete brain regions and future studies must test the molecular alterations in different brain structures to determine whether these changes are universal or

brain region-specific. Second, all the neurochemical characterizations have been performed at the end of CBDV treatment, when the compound was still effective in recovering cognitive deficits but no longer beneficial towards neurological and motor signs. Thus, it cannot be excluded that different modifications could have been observed as a consequence of CBDV administration if the same analysis would have been carried out at earlier time points (i.e. at 7 weeks of age when CBDV showed efficacy also towards neurological and motor signs). Accordingly, when biochemical investigations were performed at an early symptomatic stage of the disease they failed to reveal any defect on BDNF and IGF1 levels as well as on the phosphorylation level of the rpS6 in the brain of *MeCP2*-308 mice treated with either vehicle or CBDV (Vigli et al., 2018). Importantly, our data obtained at this advanced stage of the disease highlight that CBDV treatment can normalize BDNF/IGF1 levels as well as the defective PI3K/AKT/mTOR pathway in *Mecp2* mutant mice, possibly contributing to the restoration of cognitive deficits. Despite these limitations, this paper demonstrate that chronic CBDV administration exerts an enduring and complete rescue of recognition memory deficits in *Mecp2* mutant mice, an effect that is associated with the normalization of BDNF, IGF-1 and rpS6 phosphorylation levels as well as CB1 and CB2 receptor expression. Regarding neurological and motor signs, our data support previous findings indicating that CBDV can ameliorate neurological and motor

signs during an early symptomatic phase of the disease (Vigli et al., 2018) but highlight that this effect is only transient and is lost at advanced stages of the phenotype progression.

As a whole, available evidence encourages the investigation of the molecular mechanism(s) by which CBDV can affect behavioral and molecular parameters in this animal model as well as a more specific evaluation of CBDV's efficacy in female models of RTT-like symptoms.

Funding

This work was funded by GW Research Ltd. (Cambridge, UK). NL and CKN are indebted to the Italian association of parents proRETT research for their continuous economical support and faith in our work. EZ has a postdoctoral fellowship from Zardi Gori Foundation (Milan, Italy).

Declaration of conflicting interests

JSB and MW are employees of GW Research Ltd. (Cambridge, UK). DP, FP, TR and VD receive research grants from GW Research Ltd. All other authors declare no conflicts of interest.

References

Amada N, Yamasaki Y, Williams CM, Whalley BJ (2013) Cannabidivarin (CBDV) suppresses pentylenetetrazole (PTZ)-induced increases in epilepsy-related gene expression. PeerJ 1: e214.

Amir RE, Van den Veyver IB, Wan M, Tran CQ, Francke U, Zoghbi HY (1999) Rett syndrome is caused by mutations in X-linked MECP2, encoding methyl-CpG-binding protein 2. Nat Genet 23(2): 185-188.

Avraham Y, Grigoriadis N, Poutahidis T, Vorobiev L, Magen I, Ilan Y, Mechoulam R, Berry E (2011) Cannabidiol improves brain and liver function in a fulminant hepatic failure-induced model of hepatic encephalopathy in mice. Br J Pharmacol 162(7):1650-1658.

Bisogno T, Howell F, Williams G, Minassi A, Cascio MG, Ligresti A, Matias I, Schiano-Moriello A, Paul P, Williams EJ, Gangadharan U, Hobbs C, Di Marzo V, Doherty P (2003) Cloning of the first sn1-DAG lipases points to the spatial and temporal regulation of endocannabinoid signaling in the brain. J Cell Biol 163(3): 463-468.

Busquets-Garcia A, Gomis-González M, Guegan T, Agustín-Pavón C, Pastor A, Mato S, Pérez-Samartín A, Matute C, de la Torre R, Dierssen M, Maldonado R, Ozaita A (2013) Targeting the endocannabinoid system in the treatment of fragile X syndrome. Nat Med 19(5):603-607.

Campolongo P, Trezza V (2012) The endocannabinoid system: a key modulator of emotions and cognition. Front Behav Neurosci 6:73.

Campos AC, Fogaça MV, Scarante FF, Joca SRL, Sales AJ, Gomes FV, Sonego AB, Rodrigues NS, Galve-Roperh I, Guimarães FS (2017) Plastic

and Neuroprotective Mechanisms Involved in the Therapeutic Effects of Cannabidiol in Psychiatric Disorders. Front Pharmacol 8:269.

Campos AC, Fogaca MV, Sonego AB, Guimaraes FS (2016) Cannabidiol, neuroprotection and neuropsychiatric disorders. Pharmacol Res 112: 119-127.

Chahrour M, Zoghbi HY (2007) The story of Rett syndrome: from clinic to neurobiology. Neuron 56(3): 422-437.

Chang Q, Khare G, Dani V, Nelson S, Jaenisch R (2006) The disease progression of Mecp2 mutant mice is affected by the level of BDNF expression. Neuron 49(3): 341-348.

Chen MJ, Russo-Neustadt AA (2007) Running exercise- and antidepressant-induced increases in growth and survival-associated signaling molecules are IGF-dependent. Growth Factors 25(2): 118-131.

Chen WG, Chang Q, Lin Y, Meissner A, West AE, Griffith EC, Jaenisch R, Greenberg ME (2003) Derepression of BDNF transcription involves calcium-dependent phosphorylation of MeCP2. Science 302(5646): 885-889.

Cobolli Gigli C, Scaramuzza L, Gandaglia A, Bellini E, Gabaglio M, Parolaro D, Kilstrup-Nielsen C, Landsberger N, Bedogni F (2016) MeCP2 Related Studies Benefit from the Use of CD1 as Genetic Background. PLoS One 11(4): e0153473.

Crippa JA, Guimarães FS, Campos AC, Zuardi AW (2018) Translational Investigation of the Therapeutic Potential of Cannabidiol (CBD): Toward a New Age. Front Immunol 9:2009.

De Petrocellis L, Ligresti A, Moriello AS, Allara M, Bisogno T, Petrosino S, Stott CG, Di Marzo V (2011) Effects of cannabinoids and cannabinoid-enriched Cannabis extracts on TRP channels and endocannabinoid metabolic enzymes. Br J Pharmacol 163(7): 1479-1494.

De Petrocellis L, Orlando P, Moriello AS, Aviello G, Stott C, Izzo AA, Di Marzo V (2012) Cannabinoid actions at TRPV channels: effects on TRPV3 and TRPV4 and their potential relevance to gastrointestinal inflammation. Acta Physiol (Oxf) 204(2):255-266.

Deiana S, Watanabe A, Yamasaki Y, Amada N, Arthur M, Fleming S, Woodcock H, Dorward P, Pigliacampo B, Close S, Platt B, Riedel G (2012) Plasma and brain pharmacokinetic profile of cannabidiol (CBD), cannabidivarine (CBDV), Delta(9)-tetrahydrocannabivarin (THCV) and cannabigerol (CBG) in rats and mice following oral and intraperitoneal administration and CBD action on obsessive-compulsive behaviour. Psychopharmacology (Berl) 219(3): 859-873.

Della Sala G, Putignano E, Chelini G, Melani R, Calcagno E, Michele Ratto G, Amendola E, Gross CT, Giustetto M, Pizzorusso T (2016) Dendritic Spine

Instability in a Mouse Model of CDKL5 Disorder Is Rescued by Insulin-like Growth Factor 1. Biol Psychiatry 80(4): 302-311.

Deogracias R, Yazdani M, Dekkers MP, Guy J, Ionescu MC, Vogt KE, Barde YA (2012) Fingolimod, a sphingosine-1 phosphate receptor modulator, increases BDNF levels and improves symptoms of a mouse model of Rett syndrome. Proc Natl Acad Sci U S A 109(35): 14230-14235.

Dyer AH, Vahdatpour C, Sanfeliu A, Tropea D (2016) The role of Insulin-Like Growth Factor 1 (IGF-1) in brain development, maturation and neuroplasticity. Neuroscience 325: 89-99.

Fernández-Ruiz J, Gonzáles S (2005) Cannabinoid control of motor function at the basal ganglia. Handb Exp Pharmacol (168):479-507.

Fernandez-Ruiz J, Sagredo O, Pazos MR, Garcia C, Pertwee R, Mechoulam R, Martinez-Orgado J (2013) Cannabidiol for neurodegenerative disorders: important new clinical applications for this phytocannabinoid? Br J Clin Pharmacol 75(2): 323-333.

Gadalla KK, Bailey ME, Spike RC, Ross PD, Woodard KT, Kalburgi SN, Bachaboina L, Deng JV, West AE, Samulski RJ, Gray SJ, Cobb SR (2013) Improved survival and reduced phenotypic severity following AV9/MECP2 gene transfer to neonatal and juvenile male Mecp2 knockout mice. Mol Ther 21(1): 18-30.

Gallily R, Yekhtin Z, Hanuš LO (2015) Overcoming the Bell-Shaped Dose-Response of Cannabidiol by Using Cannabis Extract Enriched in Cannabidiol. Pharmacology & Pharmacy, 6, 75-85.

Giacometti E, Luikenhuis S, Beard C, Jaenisch R (2007) Partial rescue of MeCP2 deficiency by postnatal activation of MeCP2. Proc Natl Acad Sci USA 104(6): 1931-1936.

Gomis-González M, Busquets-Garcia A, Matute C, Maldonado R, Mato S, Ozaita A (2016) Possible Therapeutic Doses of Cannabinoid Type 1 Receptor Antagonist Reverses Key Alterations in Fragile X Syndrome Mouse Model. Genes (Basel). 7(9). pii: E56.

Guy J, Gan J, Selfridge J, Cobb S, Bird A (2007) Reversal of neurological defects in a mouse model of Rett syndrome. Science 315(5815): 1143-1147.

Hagberg B (2002) Clinical manifestations and stages of Rett syndrome. Ment Retard Dev Disabil Res Rev 8(2): 61-65.

Hill AJ, Mercier MS, Hill TD, Glyn SE, Jones NA, Yamasaki Y, Futamura T, Duncan M, Stott CG, Stephens GJ, Williams CM, Whalley BJ (2012a) Cannabidivarin is anticonvulsant in mouse and rat. Br J Pharmacol 167(8): 1629-1642.

Hill AJ, Williams CM, Whalley BJ, Stephens GJ (2012b) Phytocannabinoids as novel therapeutic agents in CNS disorders. Pharmacol Ther 133(1): 79-97.

Hill TD, Cascio MG, Romano B, Duncan M, Pertwee RG, Williams CM, Whalley BJ, Hill AJ (2013) Cannabidivarin-rich cannabis extracts are anticonvulsant in mouse and rat via a CB1 receptor-independent mechanism. Br J Pharmacol 170(3): 679-692.

Hosie S, Malone DT, Liu S, Glass M, Adlard PA, Hannan AJ, Hill-Yardin EL (2018) Altered Amygdala Excitation and CB1 Receptor Modulation of Aggressive Behavior in the Neuroligin-3R451C Mouse Model of Autism. Front Cell Neurosci 12:234.

Howell CJ, Sceniak MP, Lang M, Krakowiecki W, Abouelsoud FE, Lad SU, Yu H, Katz DM (2018) Activation of the Medial Prefrontal Cortex Reverses Cognitive and Respiratory Symptoms in a Mouse Model of Rett Syndrome. eNeuro 4(6).

Iannotti FA, Hill CL, Leo A, Alhusaini A, Soubrane C, Mazzarella E, Russo E, Whalley BJ, Di Marzo V, Stephens GJ (2014) Nonpsychotropic plant cannabinoids, cannabidivarin (CBDV) and cannabidiol (CBD), activate and desensitize transient receptor potential vanilloid 1 (TRPV1) channels in vitro:

potential for the treatment of neuronal hyperexcitability. ACS Chem Neurosci 5(11): 1131-1141.

Iannotti FA, Pagano E, Moriello AS, Alvino FG, Sorrentino NC, D'Orsi L, Gazzerro E, Capasso R, De Leonibus E, De Petrocellis L, Di Marzo V (2018) Effects of non-euphoric plant cannabinoids on muscle quality and performance of dystrophic mdx mice. Br J Pharmacol. 2018 Aug 3. doi: 10.1111/bph.14460. [Epub ahead of print]

Johnson RA, Lam M, Punzo AM, Li H, Lin BR, Ye K, Mitchell GS, Chang Q (2012) 7,8-dihydroxyflavone exhibits therapeutic efficacy in a mouse model of Rett syndrome. J Appl Physiol (1985) 112(5): 704-710.

Jung KM, Sepers M, Henstridge CM, Lassalle O, Neuhofer D, Martin H, Ginger M, Frick A, DiPatrizio NV, Mackie K, Katona I, Piomelli D, Manzoni OJ (2012) Uncoupling of the endocannabinoid signalling complex in a mouse model of fragile X syndrome. Nat Commun 3:1080.

Karhson DS, Hardan AY, Parker KJ (2016) Endocannabinoid signaling in social functioning: an RDoC perspective. Transl Psychiatry 6(9): e905.

Karhson DS, Krasinska KM, Dallaire JA, Libove RA, Phillips JM, Chien AS, Garner JP, Hardan AY, Parker KJ (2018) Plasma anandamide concentrations are lower in children with autism spectrum disorder. Mol Autism 9:18.

Katona I (2015) Cannabis and Endocannabinoid Signaling in Epilepsy. Handb Exp Pharmacol 231: 285-316.

Kerr DM, Gilmartin A, Roche M (2016) Pharmacological inhibition of fatty acid amide hydrolase attenuates social behavioural deficits in male rats prenatally exposed to valproic acid. Pharmacol Res 113(Pt A):228-235.

Khwaja, O. S., Ho, E., Barnes, K. V., O'Leary, H. M., Pereira, L. M., Finkelstein, Y., Nelson, C. A., 3rd, Vogel-Farley, V., DeGregorio, G., Holm, I. A., Khatwa, U., Kapur, K., Alexander, M. E., Finnegan, D. M., Cantwell, N. G., Walco, A. C., Rappaport, L., Gregas, M., Fichorova, R. N., Shannon, M. W., Sur, M., Kaufmann, W. E., 2014. Safety, pharmacokinetics, and preliminary assessment of efficacy of mecasermin (recombinant human IGF-1) for the treatment of Rett syndrome. Proc Natl Acad Sci U S A 111, 4596-4601.

Kron, M., Lang, M., Adams, I. T., Sceniak, M., Longo, F., Katz, D. M., 2014. A BDNF loop-domain mimetic acutely reverses spontaneous apneas and respiratory abnormalities during behavioral arousal in a mouse model of Rett syndrome. Dis Model Mech 7, 1047-1055.

Li, W., Pozzo-Miller, L., 2014. BDNF deregulation in Rett syndrome. Neuropharmacology 76 Pt C, 737-746.

Ligresti, A., De Petrocellis, L., Di Marzo, V., 2016. From Phytocannabinoids to Cannabinoid Receptors and Endocannabinoids: Pleiotropic Physiological and Pathological Roles Through Complex Pharmacology. Physiol Rev 96, 1593-1659.

Magen I, Avraham Y, Ackerman Z, Vorobiev L, Mechoulam R, Berry EM (2010) Cannabidiol ameliorates cognitive and motor impairments in bile-duct ligated mice via 5-HT1A receptor activation. Br J Pharmacol 159(4):950-957.

Martinowich, K., Hattori, D., Wu, H., Fouse, S., He, F., Hu, Y., Fan, G., Sun, Y. E., 2003. DNA methylation-related chromatin remodeling in activity-dependent BDNF gene regulation. Science 302, 890-893.

Nagarkatti, P., Pandey, R., Rieder, S. A., Hegde, V. L., Nagarkatti, M., 2009. Cannabinoids as novel anti-inflammatory drugs. Future Med Chem 1, 1333-1349.

Neul, J. L., Lane, J. B., Lee, H. S., Geerts, S., Barrish, J. O., Annese, F., Baggett, L. M., Barnes, K., Skinner, S. A., Motil, K. J., Glaze, D. G., Kaufmann, W. E., Percy, A. K., 2014. Developmental delay in Rett syndrome: data from the natural history study. J Neurodev Disord 6, 20.

Ogier, M., Wang, H., Hong, E., Wang, Q., Greenberg, M. E., Katz, D. M., 2007. Brain-derived neurotrophic factor expression and respiratory function

improve after ampakine treatment in a mouse model of Rett syndrome. J Neurosci 27, 10912-10917.

Pardridge, W. M., Kang, Y. S., Buciak, J. L., 1994. Transport of human recombinant brain-derived neurotrophic factor (BDNF) through the rat blood-brain barrier in vivo using vector-mediated peptide drug delivery. Pharm Res 11, 738-746.

Pini, G., Congiu, L., Benincasa, A., DiMarco, P., Bigoni, S., Dyer, A. H., Mortimer, N., Della-Chiesa, A., O'Leary, S., McNamara, R., Mitchell, K. J., Gill, M., Tropea, D., 2016. Illness Severity, Social and Cognitive Ability, and EEG Analysis of Ten Patients with Rett Syndrome Treated with Mecasermin (Recombinant Human IGF-1). Autism Res Treat 2016, 5073078.

Pini, G., Scusa, M. F., Benincasa, A., Bottiglioni, I., Congiu, L., Vadhatpour, C., Romanelli, A. M., Gemo, I., Puccetti, C., McNamara, R., O'Leary, S., Corvin, A., Gill, M., Tropea, D., 2014. Repeated insulin-like growth factor 1 treatment in a patient with rett syndrome: a single case study. Front Pediatr 2, 52.

Pini, G., Scusa, M. F., Congiu, L., Benincasa, A., Morescalchi, P., Bottiglioni, I., Di Marco, P., Borelli, P., Bonuccelli, U., Della-Chiesa, A., Prina-Mello, A., Tropea, D., 2012. IGF1 as a Potential Treatment for Rett Syndrome: Safety Assessment in Six Rett Patients. Autism Res Treat 2012, 679801.

R Core Team, 2013. R: A language and environment for statistical computing. R foundation for Statistical Computing, Vienna, Austria.

Ricceri, L., De Filippis, B., Laviola, G., 2008. Mouse models of Rett syndrome: from behavioural phenotyping to preclinical evaluation of new therapeutic approaches. Behav Pharmacol 19, 501-517.

Ricciardi, S., Boggio, E. M., Grosso, S., Lonetti, G., Forlani, G., Stefanelli, G., Calcagno, E., Morello, N., Landsberger, N., Biffo, S., Pizzorusso, T., Giustetto, M., Broccoli, V., 2011. Reduced AKT/mTOR signaling and protein synthesis dysregulation in a Rett syndrome animal model. Hum Mol Genet 20, 1182-1196.

Rosenthaler, S., Pohn, B., Kolmanz, C., Huu, C. N., Krewenka, C., Huber, A., Kranner, B., Rausch, W. D., Moldzio, R., 2014. Differences in receptor binding affinity of several phytocannabinoids do not explain their effects on neural cell cultures. Neurotoxicol Teratol 46, 49-56.

Roux, J. C., Zala, D., Panayotis, N., Borges-Correia, A., Saudou, F., Villard, L., 2012. Modification of Mecp2 dosage alters axonal transport through the Huntingtin/Hap1 pathway. Neurobiol Dis 45, 786-795.

Sceniak, M. P., Lang, M., Enomoto, A. C., James Howell, C., Hermes, D. J., Katz, D. M., 2016. Mechanisms of Functional Hypoconnectivity in the Medial Prefrontal Cortex of Mecp2 Null Mice. Cereb Cortex 26, 1938-1956.

Schmid, D. A., Yang, T., Ogier, M., Adams, I., Mirakhur, Y., Wang, Q., Massa, S. M., Longo, F. M., Katz, D. M., 2012. A TrkB small molecule partial agonist rescues TrkB phosphorylation deficits and improves respiratory function in a mouse model of Rett syndrome. J Neurosci 32, 1803-1810.

Sciolino, N. R., Bortolato, M., Eisenstein, S. A., Fu, J., Oveisi, F., Hohmann, A. G., Piomelli, D., 2010. Social isolation and chronic handling alter endocannabinoid signaling and behavioral reactivity to context in adult rats. Neuroscience 168, 371-386.

Servadio M, Melancia F, Manduca A, di Masi A, Schiavi S, Cartocci V, Pallottini V, Campolongo P, Ascenzi P, Trezza V (2016) Targeting anandamide metabolism rescues core and associated autistic-like symptoms in rats prenatally exposed to valproic acid. Transl Psychiatry 6:e902.

Szczesna, K., de la Caridad, O., Petazzi, P., Soler, M., Roa, L., Saez, M. A., Fourcade, S., Pujol, A., Artuch-Iriberri, R., Molero-Luis, M., Vidal, A., Huertas, D., Esteller, M., 2014. Improvement of the Rett syndrome phenotype in a MeCP2 mouse model upon treatment with levodopa and a dopa-decarboxylase inhibitor. Neuropsychopharmacology 39, 2846-2856.

Tropea, D., Giacometti, E., Wilson, N. R., Beard, C., McCurry, C., Fu, D. D., Flannery, R., Jaenisch, R., Sur, M., 2009. Partial reversal of Rett Syndrome-

like symptoms in MeCP2 mutant mice. Proc Natl Acad Sci U S A 106, 2029-2034.

Tropea, D., Kreiman, G., Lyckman, A., Mukherjee, S., Yu, H., Horng, S., Sur, M., 2006. Gene expression changes and molecular pathways mediating activity-dependent plasticity in visual cortex. Nat Neurosci 9, 660-668.

Vigli, D., Cosentino, L., Raggi, C., Laviola, G., Woolley-Roberts, M., De Filippis, B., 2018. Chronic treatment with the phytocannabinoid Cannabidivarin (CBDV) rescues behavioural alterations and brain atrophy in a mouse model of Rett syndrome. Neuropharmacology 140, 121-129.

Volkow ND, Baler RD, Compton WM, Weiss SR (2014) Adverse health effects of marijuana use. N Engl J Med. 370(23):2219-2227.

Wei D, Allsop S, Tye K, Piomelli D (2017) Endocannabinoid signaling in the control of social behavior. Trends Neurosci 40(7): 385-396.

Wei D, Dinh D, Lee D, Li D, Anguren A, Moreno-Sanz G, Gall CM, Piomelli D (2016) Enhancement of Anandamide-Mediated Endocannabinoid Signaling Corrects Autism-Related Social Impairment. Cannabis Cannabinoid Res 1(1): 81-89.

Yoshii, A., Constantine-Paton, M., 2007. BDNF induces transport of PSD-95 to dendrites through PI3K-AKT signaling after NMDA receptor activation. Nat Neurosci 10, 702-711.

Zamberletti E, Gabaglio M, Parolaro D (2017) The Endocannabinoid System and Autism Spectrum Disorders: Insights from Animal Models. Int J Mol Sci 18(9). pii: E1916.

Zamberletti, E., Gabaglio, M., Prini, P., Rubino, T., Parolaro, D., 2015. Cortical neuroinflammation contributes to long-term cognitive dysfunctions following adolescent delta-9-tetrahydrocannabinol treatment in female rats. Eur Neuropsychopharmacol 25, 2404-2415.

Zhang, J., Hu, M., Teng, Z., Tang, Y., Chen, C., 2014. Synaptic and Cognitive Improvements by Inhibition of 2-AG Metabolism Are through Upregulation of MicroRNA-188-3p in a Mouse Model of Alzheimer's Disease. J Neurosci 34, 14919-14933.

Zheng, W. H., Quirion, R., 2004. Comparative signaling pathways of insulin-like growth factor-1 and brain-derived neurotrophic factor in hippocampal neurons and the role of the PI3 kinase pathway in cell survival. J Neurochem 89, 844-852.

Zuardi AW, Rodrigues NP, Silva AL, Bernardo SA, Hallak JEC, Guimarães FS, Crippa JAS (2017) Inverted U-Shaped Dose-Response Curve of the Anxiolytic Effect of Cannabidiol during Public Speaking in Real Life. Front Pharmacol 8:259.

Figure legends

Figure 1: Effect of chronic CBDV (0.2, 2, 20, 200 mg/kg/day, weeks 5-9) treatment on the *Mecp2* KO phenotype. (**A**) “Score Test” for tremor, hindlimb clasping, breathing, gait, mobility and general condition in *Mecp2* KO mice. Animals were scored (from 0 to 2) every other day and score data represent the weekly average of four-day observations in each corresponding week for each symptom considered. (**B**) Total symptom scores in vehicle- and CBDV-treated *Mecp2* KO mice. Data represent mean ± SEM of 22 WT-vehicle, 10 WT-CBDV 0.2 mg/kg, 13 WT-CBDV 2 mg/kg, 12 WT-CBDV 20 mg/kg, 3 WT-CBDV 200 mg/kg, 11 KO-vehicle, 6 KO-CBDV 0.2 mg/kg, 13 KO-CBDV 2 mg/kg, 14 KO-CBDV 20 mg/kg, 8 KO-CBDV 200 mg/kg and were analyzed using Pearson’s Chi square test with Yates correction. *p<0.05, **p<0.01, ***p<0.001 vs KO-vehicle mice.

Figure 2: (**A**) Effect of chronic CBDV (0.2, 2, 20, 200 mg/kg/day, weeks 5-9) treatment on survival in *Mecp2* KO mice. Kaplan-Meier survival curves of CBDV-treated *Mecp2* KO mice compared to KO-vehicle littermates (p=0.0183, Kaplan–Meier log-rank test). The table summarizes the n number of KO mice in each considered week. (**B**) Area under the curve (AUC) for body weight recorded daily during the whole treatment schedule. Data are expressed as mean ± SEM 22 WT-vehicle, 10 WT-CBDV 0.2 mg/kg, 13 WT-CBDV 2 mg/kg, 12 WT-CBDV 20

mg/kg, 3 WT-CBDV 200 mg/kg, 11 KO-vehicle, 6 KO-CBDV 0.2 mg/kg, 13 KO-CBDV 2 mg/kg, 14 KO-CBDV 20 mg/kg, 8 KO-CBDV 200 mg/kg and were analyzed using a two-way ANOVA followed by Tukey's multiple comparison test. *p<0.05 vs WT-vehicle mice.

Figure 3: Effect of chronic CBDV (0.2, 2, 20, 200 mg/kg/day, weeks 5-9) treatment on recognition memory in WT and KO mice as measured through the NOR test at PND 41, 56 and 66. Data are expressed as mean ± S.E.M. of 22 WT-vehicle, 10 WT-CBDV 0.2 mg/kg, 13 WT-CBDV 2 mg/kg, 12 WT-CBDV 20 mg/kg, 3 WT-CBDV 200 mg/kg, 11 KO-vehicle, 6 KO-CBDV 0.2 mg/kg, 13 KO-CBDV 2 mg/kg, 14 KO-CBDV 20 mg/kg, 8 KO-CBDV 200 mg/kg and were analyzed by two-way repeated measures ANOVA (genotype and treatment as between factors and time as within factor) followed by Tukey's multiple comparison test. *p<0.05, **p<0.01, ***p<0.001 vs WT-vehicle; °°°p<0.001 vs KO-vehicle.

Figure 4: Effect of chronic CBDV treatment on protein levels of (**A**) BDNF and IGF-1, and (**B**) p-Akt (Ser473), its downstream effector p-rpS6 (Ser240/244), and ERK1/2 phosphorylation in the brains of *Mecp2* WT and KO mice. Measurements were carried out on total protein lysates from hemisected brains. Representative blot images correspond to the results of one experiment out of four. Data are expressed as mean ± SEM of 3-5 animals per group and were analyzed by two-way ANOVA followed by Tukey's multiple comparison test. *p<0.05, **p<0.01,

***p<0.001 vs WT-vehicle; °p<0.05, °°p<0.01; °°°p<0.001 vs KO-vehicle. (**C**) n. of p-rpS6(Ser240/244)-positive neurons in layer V of the mPFC as quantified through immunohistochemistry. Data represent mean ± SEM of three animals per each experimental group (four slices /animal) and were analyzed by two-way ANOVA followed by Tukey's multiple comparison test. *p<0.05 vs WT-vehicle; °p<0.05, °°p<0.01 vs KO-vehicle. (**D**) Representative high magnification (40x) views of p-rpS6 (Ser240/244) immunolabeling in layer V neurons of the mPFC in 9-week-old *Mecp2* WT and KO animals either treated with vehicle of CBDV (Scale bar = 50μm).

Figure 5: Nuclear volume measurements of DAPI-labeled nuclei in the layer V of the mPFC (**A**) and (**B**) CA1 region of the hippocampus in *Mecp2* KO and WT mice after chronic CBDV administration. Bar plots show mean nuclear volumes ± SEM of three animals per each experimental group (four slices/30-75 cells/animal). Statistical analysis was carried out by two-way ANOVA and Tukey's multiple comparison test. *p<0.05, **p<0.01, ***p<0.001 vs WT-vehicle; °p<0.05 vs KO-vehicle.

Figure 6: Effect of chronic CBDV treatment on (**A**) protein levels of CB1 and CB2 cannabinoid receptors in hemisected brains of *Mecp2* WT and KO mice. (**B**) Representative blot images correspond to the results of one experiment out of four. Data are expressed as mean ± SEM of 3-6 animals per group and were

analyzed by two-way ANOVA followed by Tukey's multiple comparison test. *p<0.05, **p<0.01, ***p<0.001 vs WT-vehicle; °p<0.05, °°p<0.01; °°°p<0.001 vs KO-vehicle.

Figure 7: Effect of chronic CBDV treatment on (**A**) AEA, 2-AG, PEA and OEA contents and (**B**) protein levels of the main endocannabinoid synthetic and degrading enzymes NAPE-PLD, DAGLα, FAAH and MAGL in hemisected brains of *Mecp2* WT and KO mice. Representative blot images correspond to the results of one experiment out of four. Data are expressed as mean ± SEM of 3-6 animals per group and analyzed by two-way ANOVA followed by Tukey's multiple comparison test. *p<0.05, **p<0.01, ***p<0.001 vs WT-vehicle; °p<0.05, °°p<0.01; °°°p<0.001 vs KO-vehicle.

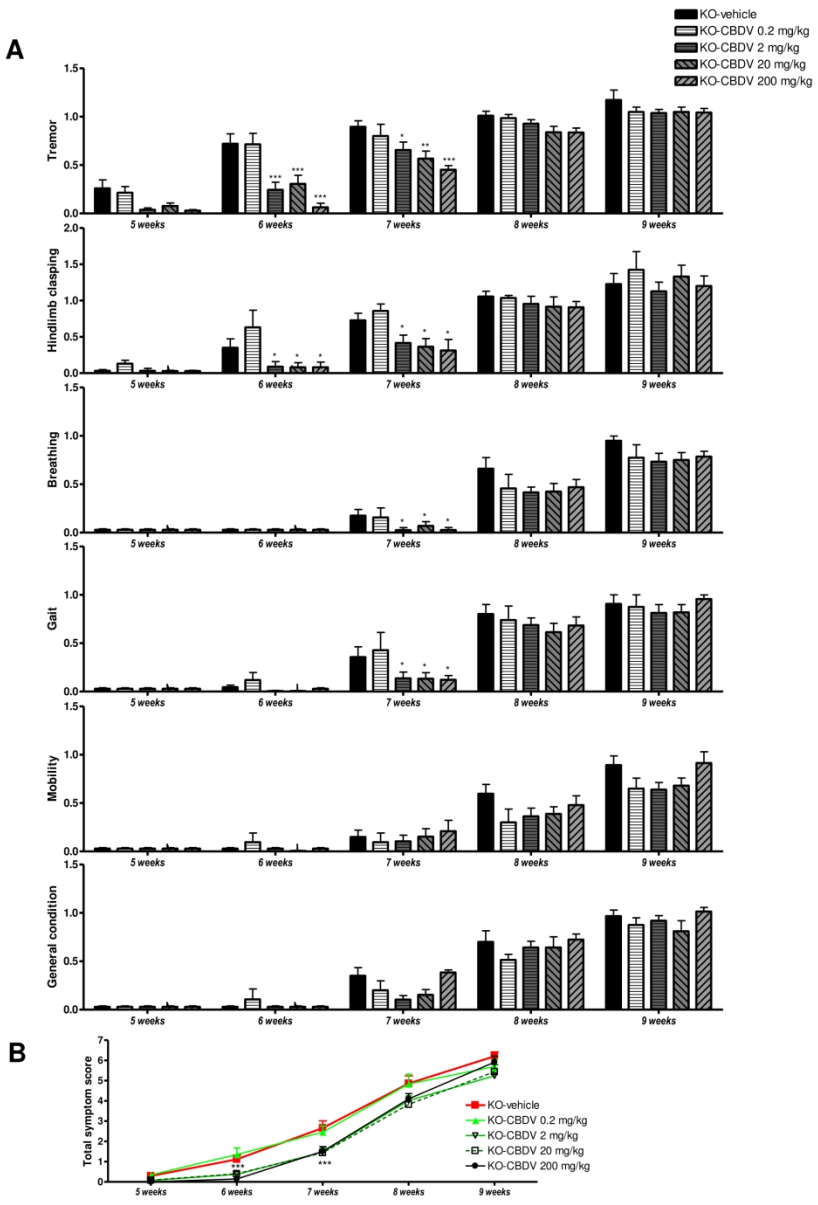

Figure 1: Effect of chronic CBDV (0.2, 2, 20, 200 mg/kg/day, weeks 5-9) treatment on the Mecp2 KO phenotype. (A) "Score Test" for tremor, hindlimb clasping, breathing, gait, mobility and general condition in Mecp2 KO mice. Animals were scored (from 0 to 2) every other day and score data represent the weekly average of four-day observations in each corresponding week for each symptom considered. (B) Total symptom scores in vehicle- and CBDV-treated Mecp2 KO mice. Data represent mean ± SEM of 22 WT-vehicle, 10 WT-CBDV 0.2 mg/kg, 13 WT-CBDV 2 mg/kg, 12 WT-CBDV 20 mg/kg, 3 WT-CBDV 200 mg/kg, 11 KO-vehicle, 6 KO-CBDV 0.2 mg/kg, 13 KO-CBDV 2 mg/kg, 14 KO-CBDV 20 mg/kg, 8 KO-CBDV 200 mg/kg and were analyzed using Pearson's Chi square test with Yates correction. *p<0.05, **p<0.01, ***p<0.001 vs KO-vehicle mice.

812x1058mm (72 x 72 DPI)

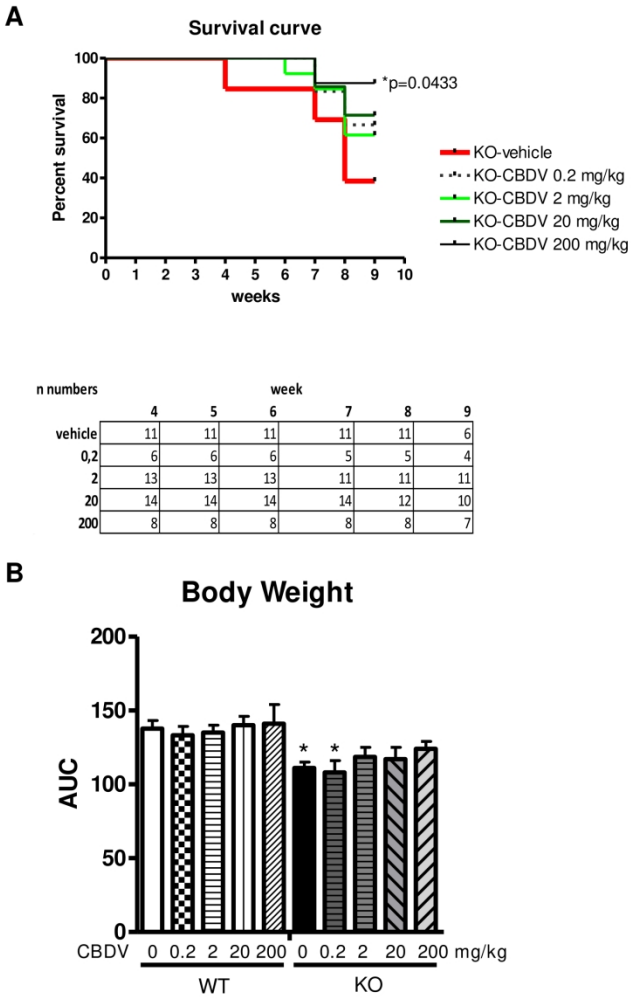

Figure 2: (A) Effect of chronic CBDV (0.2, 2, 20, 200 mg/kg/day, weeks 5-9) treatment on survival in Mecp2 KO mice. Kaplan-Meier survival curves of CBDV-treated Mecp2 KO mice compared to KO-vehicle littermates (p=0.0183, Kaplan–Meier log-rank test). The table summarizes the n number of KO mice in each considered week. (B) Area under the curve (AUC) for body weight recorded daily during the whole treatment schedule. Data are expressed as mean ± SEM 22 WT-vehicle, 10 WT-CBDV 0.2 mg/kg, 13 WT-CBDV 2 mg/kg, 12 WT-CBDV 20 mg/kg, 3 WT-CBDV 200 mg/kg, 11 KO-vehicle, 6 KO-CBDV 0.2 mg/kg, 13 KO-CBDV 2 mg/kg, 14 KO-CBDV 20 mg/kg, 8 KO-CBDV 200 mg/kg and were analyzed using a two-way ANOVA followed by Tukey's multiple comparison test. *p<0.05 vs WT-vehicle mice.

812x1058mm (72 x 72 DPI)

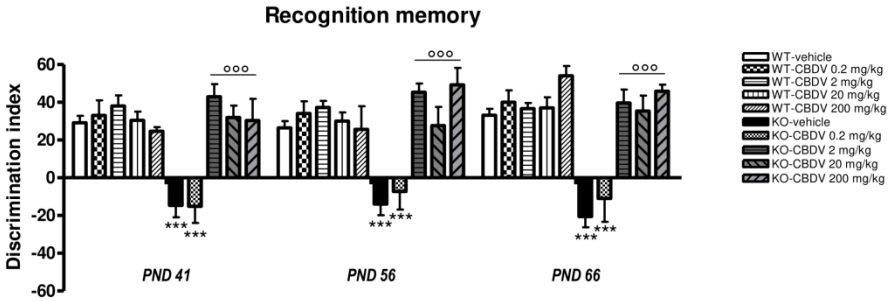

Figure 3: Effect of chronic CBDV (0.2, 2, 20, 200 mg/kg/day, weeks 5-9) treatment on recognition memory in WT and KO mice as measured through the NOR test at PND 41, 56 and 66. Data are expressed as mean ± S.E.M. of 22 WT-vehicle, 10 WT-CBDV 0.2 mg/kg, 13 WT-CBDV 2 mg/kg, 12 WT-CBDV 20 mg/kg, 3 WT-CBDV 200 mg/kg, 11 KO-vehicle, 6 KO-CBDV 0.2 mg/kg, 13 KO-CBDV 2 mg/kg, 14 KO-CBDV 20 mg/kg, 8 KO-CBDV 200 mg/kg and were analyzed by two-way repeated measures ANOVA (genotype and treatment as between factors and time as within factor) followed by Tukey's multiple comparison test. *p<0.05, **p<0.01, ***p<0.001 vs WT-vehicle; °°°p<0.001 vs KO-vehicle.

829x418mm (72 x 72 DPI)

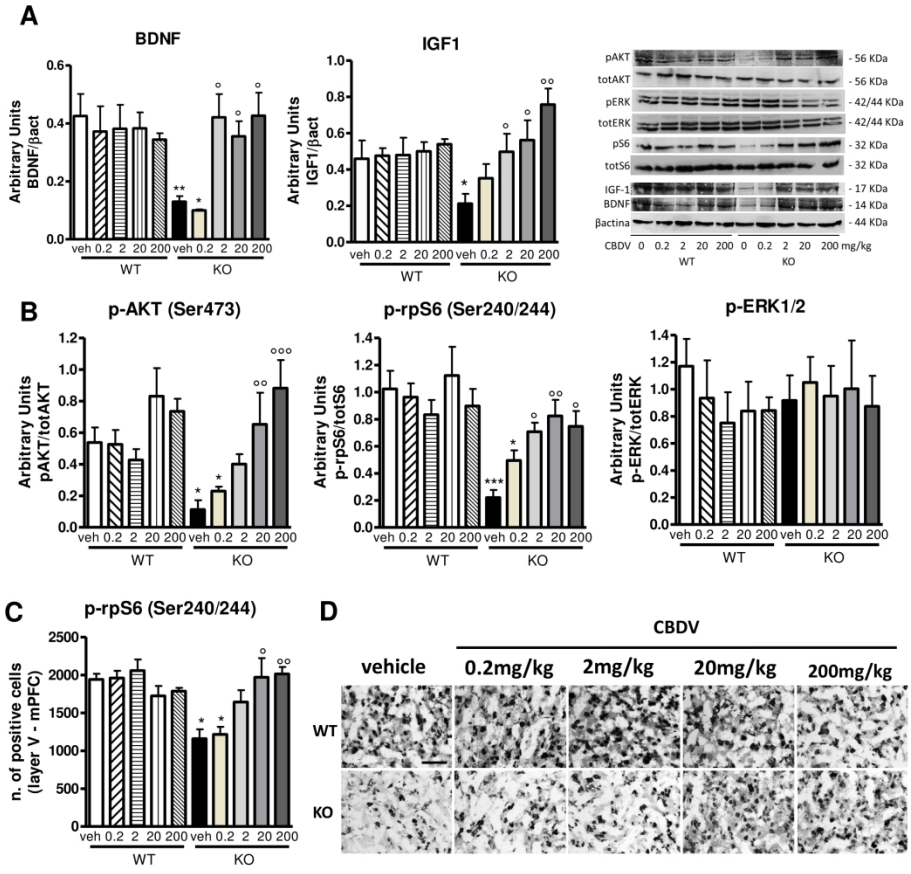

Figure 4: Effect of chronic CBDV treatment on protein levels of (A) BDNF and IGF-1, and (B) p-Akt (Ser473), its downstream effector p-rpS6 (Ser240/244), and ERK1/2 phosphorylation in the brains of Mecp2 WT and KO mice. Measurements were carried out on total protein lysates from hemisected brains. Representative blot images correspond to the results of one experiment out of four. Data are expressed as mean ± SEM of 3-5 animals per group and were analyzed by two-way ANOVA followed by Tukey's multiple comparison test. *p<0.05, **p<0.01, ***p<0.001 vs WT-vehicle; °p<0.05, °°p<0.01; °°°p<0.001 vs KO-vehicle. (C) n. of p-rpS6(Ser240/244)-positive neurons in layer V of the mPFC as quantified through immunohistochemistry. Data represent mean ± SEM of three animals per each experimental group (four slices /animal) and were analyzed by two-way ANOVA followed by Tukey's multiple comparison test. *p<0.05 vs WT-vehicle; °p<0.05, °°p<0.01 vs KO-vehicle. (D) Representative high magnification (40x) views of p-rpS6 (Ser240/244) immunolabeling in layer V neurons of the mPFC in 9-week-old Mecp2 WT and KO animals either treated with vehicle of CBDV (Scale bar = 50μm).

812x1058mm (72 x 72 DPI)

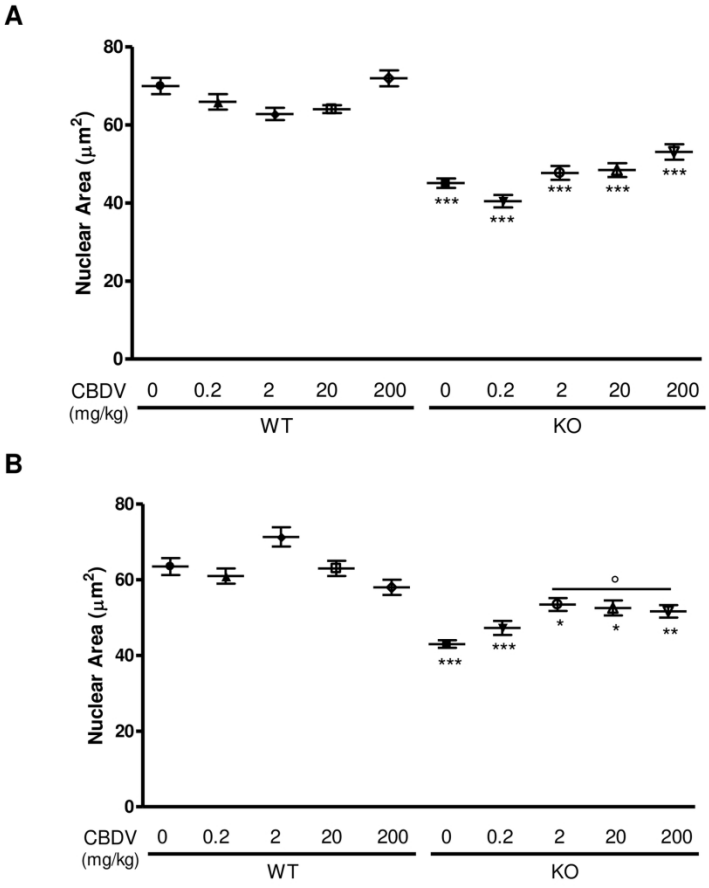

Figure 5: Nuclear volume measurements of DAPI-labeled nuclei in the layer V of the mPFC (A) and (B) CA1 region of the hippocampus in Mecp2 KO and WT mice after chronic CBDV administration. Bar plots show mean nuclear volumes ± SEM of three animals per each experimental group (four slices/30-75 cells/animal). Statistical analysis was carried out by two-way ANOVA and Tukey's multiple comparison test. *p<0.05, **p<0.01, ***p<0.001 vs WT-vehicle; °p<0.05 vs KO-vehicle.

194x254mm (300 x 300 DPI)

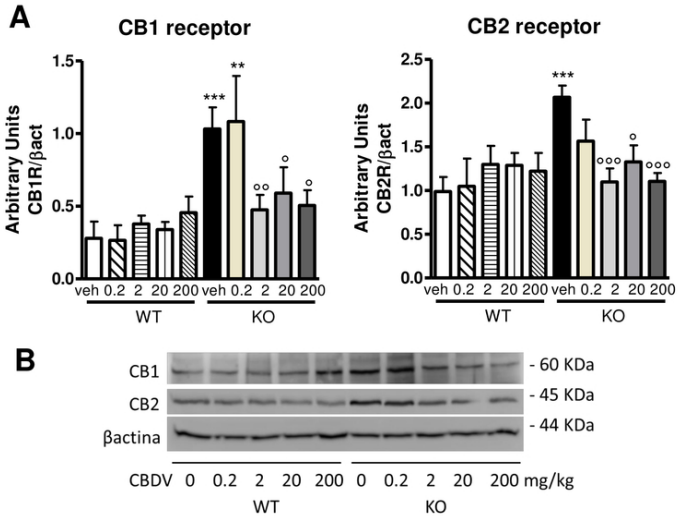

Figure 6: Effect of chronic CBDV treatment on (A) protein levels of CB1 and CB2 cannabinoid receptors in hemisected brains of Mecp2 WT and KO mice. (B) Representative blot images correspond to the results of one experiment out of four. Data are expressed as mean ± SEM of 3-6 animals per group and were analyzed by two-way ANOVA followed by Tukey's multiple comparison test. *p<0.05, **p<0.01, ***p<0.001 vs WT-vehicle; °p<0.05, °°p<0.01; °°°p<0.001 vs KO-vehicle.

91x63mm (300 x 300 DPI)

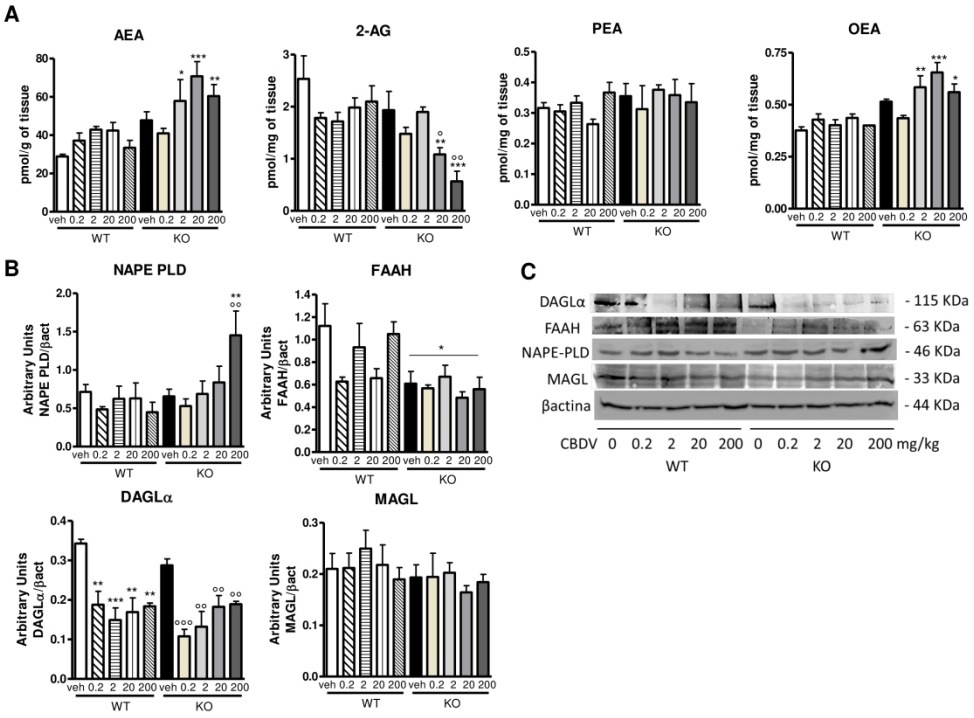

Figure 7: Effect of chronic CBDV treatment on (A) AEA, 2-AG, PEA and OEA contents and (B) protein levels of the main endocannabinoid synthetic and degrading enzymes NAPE-PLD, DAGLα, FAAH and MAGL in hemisected brains of Mecp2 WT and KO mice. Representative blot images correspond to the results of one experiment out of four. Data are expressed as mean ± SEM of 3-6 animals per group and analyzed by two-way ANOVA followed by Tukey's multiple comparison test. *p<0.05, **p<0.01, ***p<0.001 vs WT-vehicle; °p<0.05, °°p<0.01; °°°p<0.001 vs KO-vehicle.

Supplementary Methods

Score test

Mecp2 WT and KO mice were scored every other day to evaluate the effect of CBDV treatment on Hindlimb clasping, gait, breathing, tremor, mobility and general condition. Each of the six symptoms was scored from 0 to 2 (0 corresponds to the symptom being absent or the same as in the WT animal; 1 when the symptom was present; 2 when the symptom was severe). Specifically: For tremor: the mouse was observed while standing on the flat palm of the hand. 0 = no tremor; 1 = intermittent mild tremor; 2 = continuous tremor or intermittent violent tremor. For hind limb clasping: 0 = WT; hind limbs splay outward when suspended by the tail; 1 = one hind limb is pulled into the body or forelimbs are stiff and splayed outward without motion; and 2 = one hind limb is pulled into the body and forelimbs are stiff and splayed outward without motion and might form a widened bowl shape or both hind limbs are pulled into the body with or without abnormal forelimb posture. For breathing: movement of flanks were observed while the animal was standing still. 0 = normal breathing; 1 = periods of regular breathing interspersed with short periods of more rapid breathing or with pauses in breathing; 2 = very irregular breathing-gasping or panting. For mobility: the mouse was observed when placed on bench, then when handled gently and scored as follows: 0 = as WT; 1 = reduced movement when compared with WT: extended freezing period when first placed on bench and longer periods spent immobile; 2 = no spontaneous movement when placed on the bench; mouse can move in response to a gentle prod or a food pellet placed nearby. For general condition: the mouse was observed for indicators of general well-being such as coat condition, eyes and body stance. 0 = clean shiny coat, clear eyes, and normal stance; 1 = eyes dull, coat dull/ungroomed, and somewhat hunched stance; 2 = eyes crusted or narrowed, piloerection, and hunched posture. For gait: 0 = as WT; 1 = hind limbs spread wider than WT when ambulating and/or a lowered pelvis when ambulating; and 2 = lack of full strides by hind limbs resulting in a dragging of hindquarters.

Table S1

	DILUITION	SUPPLIER
Rabbit polyclonal anti-BDNF	1:1000	Millipore, Italy
Goat polyclonal anti-IGF-1	1:1000	Millipore, Italy
Rabbit polyclonal anti-pAKT Ser473	1:1000	Cell Signaling, Danvers, MA
Rabbit polyclonal anti-phospho-rpS6	1:1000	Cell Signaling, Danvers, MA
Rabbit polyclonal anti-pERK1/2	1:1000	Cell Signaling, Danvers, MA
Rabbit polyclonal anti-cannabinoid CB1 receptor (CB1)	1:1000	Cayman Chemical, Ann Arbor, MI
Rabbit polyclonal anti-cannabinoid CB2 receptor (CB2)	1:1000	Cayman Chemical, Ann Arbor, MI
Rabbit polyclonal anti-N-acyl-phosphatidylethanolamine-hydrolysing phospholipase D (NAPE-PLD)	1:3000	Cayman Chemical, Ann Arbor, MI
Rabbit polyclonal anti-fatty acid amide hydrolase (FAAH)	1:2000	Cayman Chemical, Ann Arbor, MI
Goat polyclonal anti-diacylglycerol Lipase α (DAGLα)	1:1000	Abcam, Cambridge, UK
Rabbit polyclonal anti-monoacylglycerol lipase (MAGL)	1:1000	Cayman Chemical, Ann Arbor, MI

Table S1: List of primary antibodies used for Western blot analysis

Supplementary figures

Figure S1

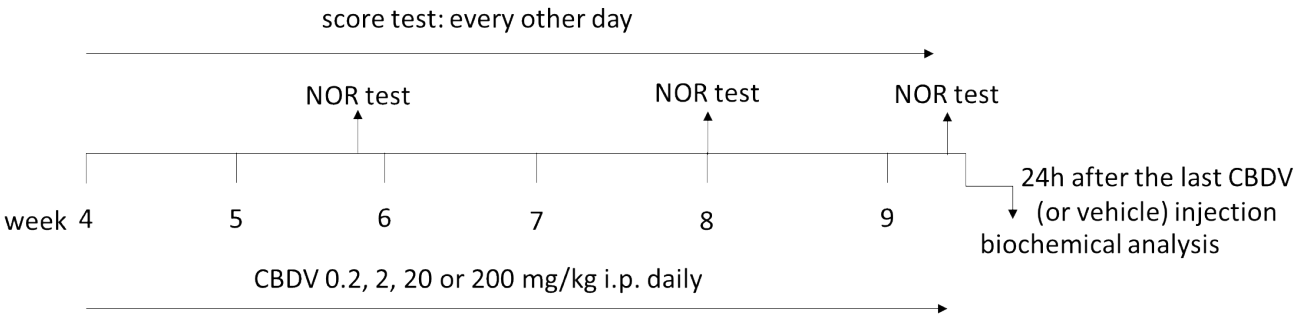

Figure S1: Timeline of the experiments

Figure S2

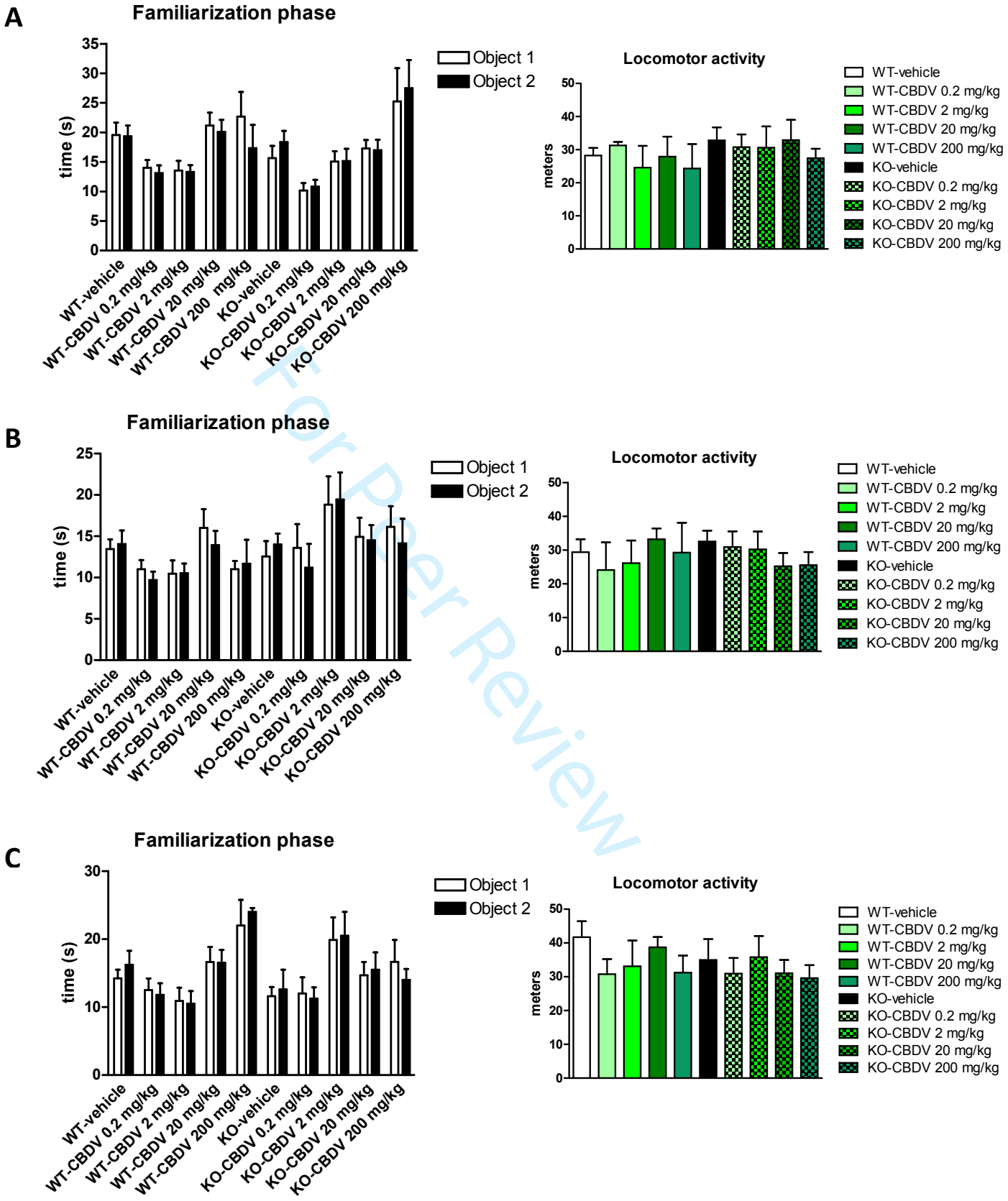

Figure S2: Exploration times and locomotor activity in vehicle- and CBDV-treated *Mecp2* WT and KO during the familiarization phase of the NOR test at PND 41 **(A)**, 56 **(B)** and 66 **(C)**. Left panels show the time spent exploring the two identical objects during the 10-minute session; right panels report total distance moved. Data are expressed as mean ± S.E.M. and analyzed using Student t test or two-way ANOVA.

Figure S3

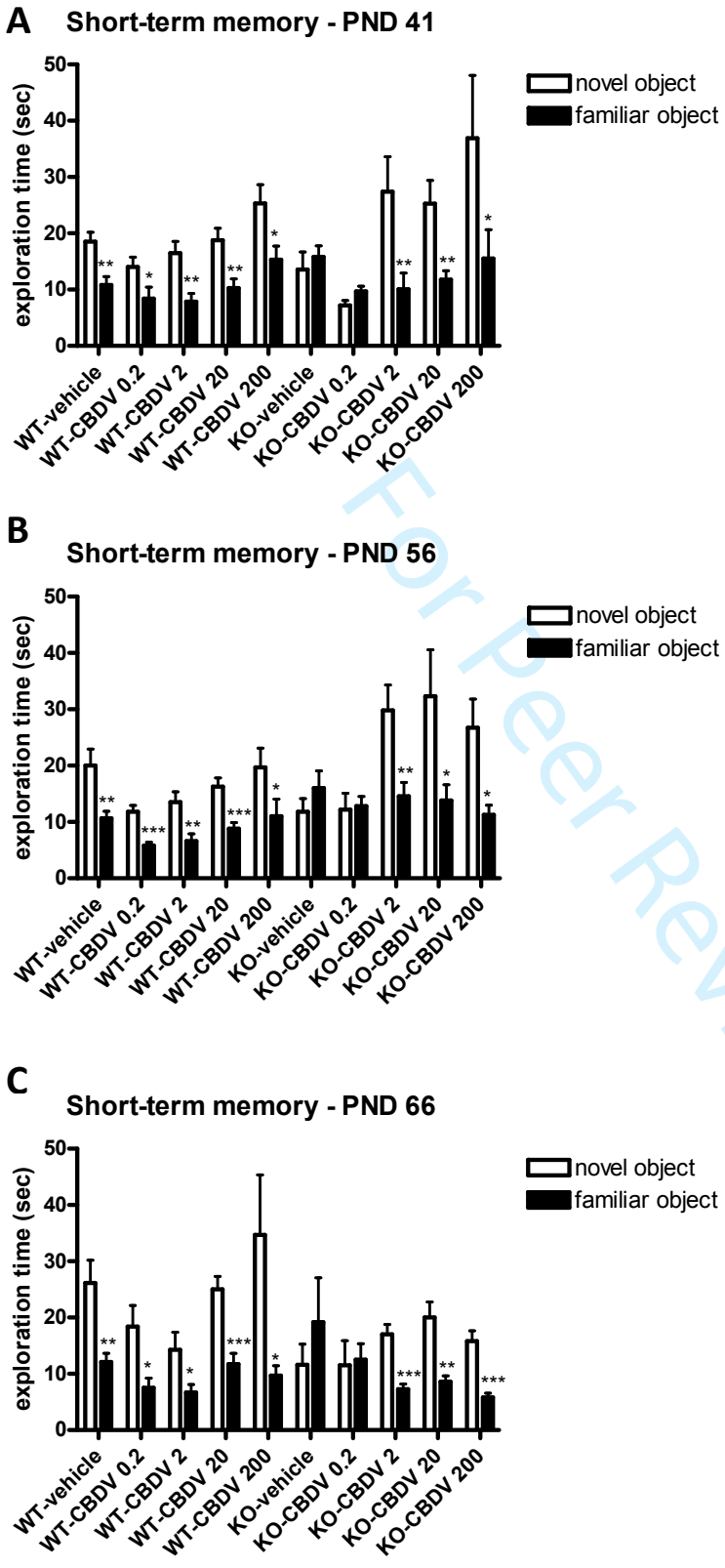

Figure S3: Exploration times of the novel object and the familiar object in vehicle- and CBDV-treated *Mecp2* WT and KO during the test phase of the NOR test at PND 41 **(A)**, 56 **(B)** and 66 **(C)**. Data are expressed as mean ± S.E.M. and analyzed using Student t test. ***p<0.001, **p<0.01, *p<0.05 vs familiar object.

Figure S4

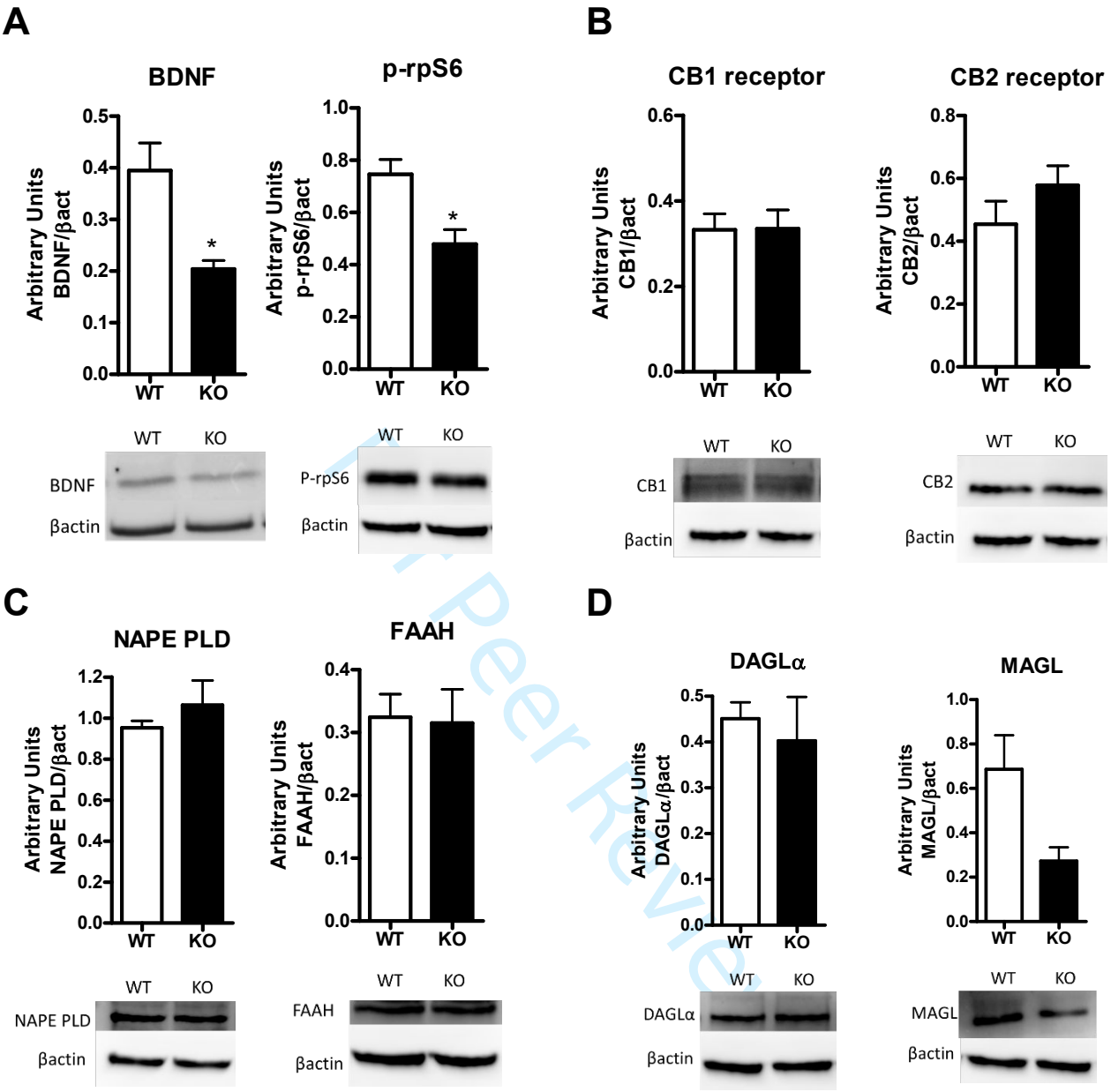

Figure S4: Protein levels of (A) BDNF and p-rpS6, (B) CB1 and CB2 receptors, (C) NAPE-PLD and FAAH, (D) DAGLα and MAGL in hemisected brains of pre-symptomatic 4-weeks-old Mecp2 WT and KO mice as measured by means of Western blot analysis. Data are expressed as mean ± S.E.M. of 4 WT and 3 KO mice per group and were analyzed using unpaired Student t test. *p<0.05 vs WT.

Figure S5

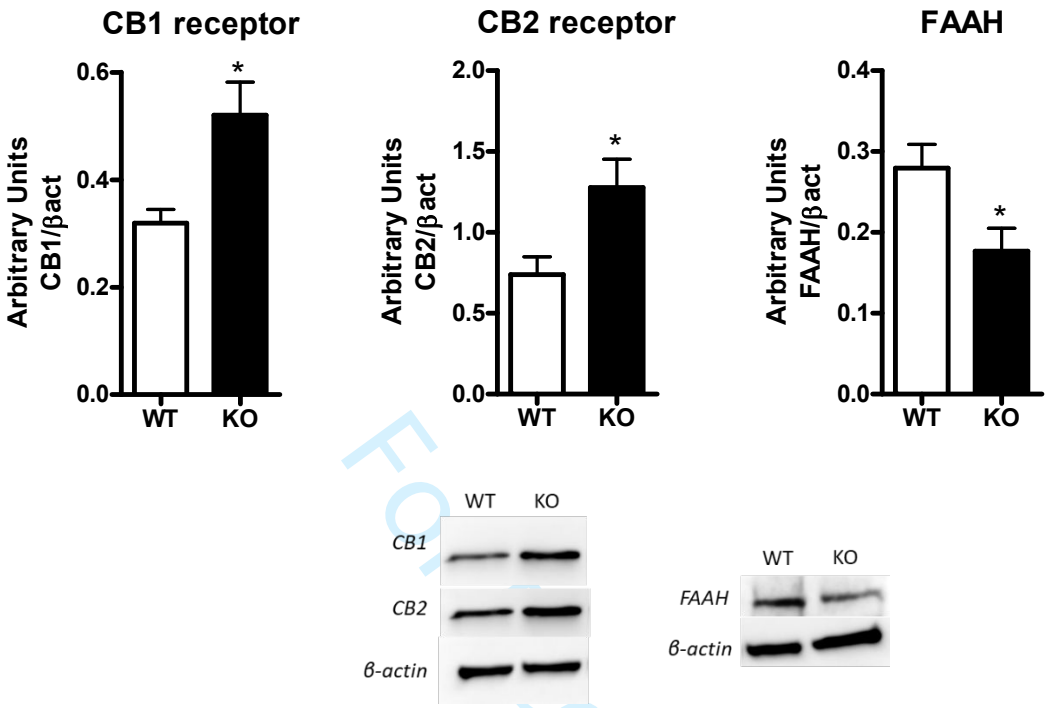

Figure S5: Protein levels of cannabinoid CB1 and CB2 receptors and FAAH in hemisected brains of naïve 9-weeks-old Mecp2 WT and KO mice (no handling) as measured by means of Western blot analysis. Data are expressed as mean ± S.E.M. of 4 mice per group and analyzed using unpaired Student t test. *p<0.05 vs WT.